COMMUN. MATH. SCI.
Vol. 21, No. 7, pp. 1895–1916

ERROR ESTIMATES OF THE SAV METHOD FOR THE COUPLED CAHN-HILLIARD SYSTEM IN COPOLYMER/HOMOPOLYMER MIXTURES*

JIN HUANG† AND GUANGHUA JI‡

Abstract. In this paper, we consider the fully discrete scheme based on the scalar auxiliary variable (SAV) approach in time and the Fourier spectral method in space, for solving the phase-field model of the blend consisting of AB diblock copolymers and C homopolymers. We establish the error estimates of the numerical scheme rigorously, and show that the fully discrete scheme converges with order $O(\tau^2+h^m)$, where τ, h, and m are the time step, spatial step and regularity of the exact solution, respectively. Finally, some numerical simulation results are presented to demonstrate the theoretical results.

Keywords. Soft confinement; copolymer/homopolymer mixtures; error estimates; nonlocal term; SAV approach.

AMS subject classifications. 35Q35; 65M12; 65N35; 76-10.

1. Introduction

In recent years, there has been tremendous interest in block copolymers (BCPs) due to their ability to produce rich nanostructures with a wide range of applications in optics and drug transport. The simplest block copolymer is the diblock copolymer, in which two types of polymer segments are covalently bound. The self-assembly behavior of diblock copolymers under confinement has attracted considerable attention [1–13]. According to the interface properties of the confined space, confinement can be divided into soft confinement and hard confinement. In a soft confined system, the interface is flexible, while in a hard confined system, it is fixed. Compared to hard confinement, soft confinement offers more possibilities for copolymer self-assembly to generate novel nanostructures [14, 16–18]. To realize soft confinement in physical experiments, researchers usually use self-organized precipitation (SORP) in which a mixture consisting of copolymers, and a third immiscible is considered [9, 15, 16]. To achieve consistency, researchers consider the copolymer/homopolymer or copolymer/solvent blend theoretically to simulate the self-assembly of block copolymers under soft confinement [17–19].

For multiphase incompressible fluids, popular modeling methods include the Monte Carlo simulated annealing method [23,24], Self-Consistent Field Theory (SCFT) [25–27], and the phase-field approach [19,28–30]. The Monte Carlo simulated annealing method is a well known procedure that seeks to obtain the lowest energy ground states of a disordered system. However, it requires a large amount of computational effort and cannot obtain the energy of the system. This problem can be partially solved by SCFT, in which the multibody interactions between polymers in the system are converted into the force of external fields. In SCFT, there is an explicit expression for free energy, but there are many coupling parameters in the SCFT equations, which results in many calculations. Similar to the previous two methods, the phase-field approach, which introduces smooth phase variables to describe the evolution of the free interface, is

---

*Received: July 23, 2022; Accepted (in revised form): January 20, 2023. Communicated by Jie Shen.

†Laboratory of Mathematics and Complex Systems (Ministry of Education), School of Mathematical Sciences, Beijing Normal University, Beijing 100875, People's Republic of China (3219810680@qq.com).

‡Laboratory of Mathematics and Complex Systems (Ministry of Education), School of Mathematical Sciences, Beijing Normal University, Beijing 100875, People's Republic of China (ghji@bnu.edu.cn).

also a popular modeling framework for polymer systems. Compared with SCFT, the phase-field approach has the advantages of fewer parameters and simpler theoretical analysis. Although the Cahn-Hilliard equations in the phase-field model are based on a small number of parameters, they are robust enough to provide guidance on the dynamic behavior of confined BCPs. For various processes involving the heating of BCP in solutions, Avalos *et al.* established a clear parameter correspondence between the temperature-dependent Flory-Huggins parameter and the width of the microphase interface [20]. Hence, we consider the phase-field approach here. The phase-field model of the copolymer/homopolymer blend was first proposed by Avalos *et al.* [21], in which novel morphologies of diblock copolymers confined in a three-dimensional sphere were obtained. Then, they simulated the phase transition from stacked lamellae to onion-like structures and gave a phase diagram containing various morphologies [20].

However, the above studies in [20, 21] focus on the simulation and prediction of physical phenomena, rather than on designing efficient algorithms for the model. In fact, solving the model efficiently is necessary and challenging because the nonlocal term in the coupled Cahn-Hilliard equations is difficult to handle properly.

For the Cahn-Hilliard equations, the common numerical methods include convex splitting [31–33], stabilization method [34–36], invariant energy quadratization (IEQ) approach [37, 38] and scalar auxiliary variable (SAV) approach [39–43]. The convex splitting method is introduced by Eyre *et al.* in [31] for time stepping the Cahn-Hilliard equations. However, it requires solving a nonlinear equation with high computational complexity at each time step. Moreover, it is difficult to construct the corresponding second-order schemes. Based on the convex splitting method, the stabilization method, which explicitly addresses nonlinear terms and adds a stability term to avoid strict time step constraints, can be extended to second-order schemes but in general it does not guarantee unconditional stability. Notably, the IEQ method, which is proposed in [37], allows us to construct linear second-order unconditionally energy stable schemes for a large class of gradient flows. However, the IEQ method often leads to variable coefficient systems, which is hard to implement. To overcome this problem, *i.e.*, constructing a numerical format that is easy to implement, Shen *et al.* proposed the SAV approach for a large class of gradient flows that describe energy dissipative physical systems [39, 40]. The schemes for gradient flows that introduce auxiliary variables are proposed for a fourth-order polynomial double well free energy in [40] and then generalized to other free energies. The related numerical studies show that the SAV method is superior to the IEQ approach [39, 41, 42] because it can inherit the advantages of the IEQ approach and overcome its shortcomings. That is, it is more efficient and easier to implement.

Compared with traditional Cahn-Hilliard equations, the key to efficiently solving the coupled Cahn-Hilliard equations lies in the treatment of nonlocal and nonlinear terms. Therefore, it is necessary to construct a nonlinear decoupled high-precision scheme for the model using the SAV method, which can guarantee unconditional energy stability. To solve this problem, Li *et al.* proposed second-order numerical schemes combining the SAV method with CN and BDF2, which are decoupled, noniterative, and easy to implement [22]. Furthermore, they demonstrated the unconditional energy stability of the SAV/CN and SAV/BDF2 schemes and pointed out that the error estimation is challenging but do not present it. The purpose of this paper is to present the error analysis for the SAV/CN scheme, which is also applicable to the SAV/BDF2 scheme.

This paper is organized as follows. In Section 2, we introduce the phase-field model of the blend consisting of AB diblock copolymers and C homopolymers. Then, we present the second-order SAV/CN scheme and the unconditional energy stability in

Section 3. The corresponding error estimate, which is guaranteed by the L^∞ bound of numerical solutions, is proved in Section 4. To verify the analysis results, we give the results of numerical simulations in two dimensions in Section 5. Finally, we present the conclusions in Section 6.

2. The model

Before introducing the phase-field model of the blend consisting of AB diblock copolymers and C homopolymers, we first introduce some notations used throughout this paper, (see, e.g., [22]). We consider a bounded domain $\Omega \in R^d, d=1,2,3$ and the usual Sobolev space denoted by $W^{s,p}(\Omega)$ $(0\le s\le\infty, 1\le p\le\infty)$. Then, we denote $H^s(\Omega):=W^{s,2}(\Omega)$ equipped with the norm $\|\cdot\|_{H^s}$ and the dual space of $H^s(\Omega)$ as $H^{-s}(\Omega)$. Furthermore, we consider the space $L^2(\Omega):=H^0(\Omega)$ associated with the inner product $(\cdot,\cdot)$ and norm $\|\cdot\|$. In particular, we define the space $L_0^2(\Omega)=\{v\in L^2(\Omega)|(v,1)=0\}$. For $f\in L_0^2(\Omega)$, we can define $v_f:=(-\Delta)^{-1}f$, where $v_f\in H^2(\Omega)\bigcap L_0^2(\Omega)$ is the unique solution of the periodic boundary value problem $-\Delta v_f=f$ in Ω. For any $f,g\in L_0^2(\Omega)$, the H^{-1} inner product and norm can be defined as

$$(f,g)_{-1}:=(\nabla v_f,\nabla v_g),\ \|f\|_{-1}:=\sqrt{(f,f)_{-1}}. \tag{2.1}$$

We denote by $f\lesssim g$ that there exists a general positive constant C such that $f\le Cg$ holds.

Here, we consider the blended system composed of AB diblock copolymers and C homopolymers in a bounded region Ω $(\Omega\in R^d,\ d=1,2,3)$. We use two order parameters (u and v) to describe macrophase separation between copolymers and homopolymers and the microphase separation between monomers A and B. u defines the state of the blend of copolymers and homopolymers, and requires values in the range of $[-1,1]$ with end points corresponding to homopolymer-rich (-1) and copolymer-rich domains (+1), respectively. v characterizes the state of AB diblock copolymers and requires values from the interval $[-1,1]$. When v takes -1 and 1, it corresponds to A-rich and B-rich domains, respectively. The total free energy takes the form [20, 21]

$$E(u,v)=\int_\Omega \frac{\epsilon_u^2}{2}|\nabla u|^2+\frac{\epsilon_v^2}{2}|\nabla v|^2+W(u,v)+\frac{\sigma}{2}|(-\triangle)^{-\frac{1}{2}}(v-\bar{v})|^2 d\mathbf{x}, \tag{2.2}$$

where parameters ϵ_u and ϵ_v are proportional to the thickness of the propagating fronts of each component. $W(u,v)=\frac{1}{4}(u^2-1)^2+\frac{1}{4}(v^2-1)^2+\alpha uv+\beta uv^2$ is the double-well potential energy, where α and β are two constants coupled with each other. $\bar{v}=\frac{1}{|\Omega|}\int_\Omega v\, d\mathbf{x}$ is the mass ratio between two polymers. The last term of E characterizes the long-range interaction between molecules in the system (related to σ) which determines that $(-\triangle)^{-\frac{1}{2}}$ must be integrated over the whole region Ω.

Using the gradient flow method, *i.e.*, taking the variational derivative of E in $H^{-1}(\Omega)$ (with respect to u and v, respectively), we obtain the conserved dynamics as follows:

$$u_t=M_u\Delta(-\epsilon_u^2\Delta u+f(u,v)), \tag{2.3}$$

$$v_t=M_v(\Delta(-\epsilon_v^2\Delta v+g(u,v))-\sigma(v-\bar{v})), \tag{2.4}$$

where M_u and M_v are mobility parameters to control the speed at which order parameters u and v move. $f(u,v)=u^3-u+\alpha v+\beta v^2$, $g(u,v)=v^3-v+\alpha u+2\beta uv$. For the Cahn-Hilliard equations, two boundary conditions can be considered: (i) periodic boundary conditions, *i.e.*, all variables are periodic on $\partial\Omega$; (ii) no-flux type boundary conditions, *i.e.*,

$$\partial_{\mathbf{n}} u|_{\partial\Omega} = \partial_{\mathbf{n}}\Delta u|_{\partial\Omega} = \partial_{\mathbf{n}} v|_{\partial\Omega} = \partial_{\mathbf{n}}\Delta v|_{\partial\Omega} = 0 \tag{2.5}$$

where $\mathbf{n}$ is the unit outward normal on $\partial\Omega$. In this work, we use periodic boundary conditions. However, our analysis is also applicable to the case of no-flux type boundary conditions.

3. Second-order SAV scheme and its stability

In the SAV approach, we first introduce a scalar variable $r = \sqrt{E_1(u,v)+C_0}$, where $E_1(u,v) = \int_\Omega (W(u,v) - \frac{S}{2}u^2 - \frac{S}{2}v^2)d\mathbf{x}$, $S \geq 0$ is a stabilization parameter, and C_0 is a positive constant to ensure $E_1(u,v)+C_0 > 0$. Therefore, the free energy functional (2.2) can be formulated as

$$E(u,v,r) = \int_\Omega (\frac{\epsilon_u^2}{2}|\nabla u|^2 + \frac{S}{2}u^2 + \frac{\epsilon_v^2}{2}|\nabla v|^2 + \frac{S}{2}v^2 + \frac{\sigma}{2}|(-\triangle)^{-\frac{1}{2}}(v-\bar{v})|^2)d\mathbf{x} + r^2 - C_0.$$

We obtain the equivalent PDE system as follows:

$$\begin{cases} u_t = M_u\Delta(-\epsilon_u^2\Delta u + Su + H(u,v)r), \\ v_t = M_v(\Delta(-\epsilon_v^2\Delta v + Sv + G(u,v)r) - \sigma(v-\bar{v})), \end{cases} \tag{3.1}$$

where

$$H(u,v) = \frac{f(u,v)-Su}{\sqrt{E_1(u,v)+C_0}},\ G(u,v) = \frac{g(u,v)-Sv}{\sqrt{E_1(u,v)+C_0}}.$$

The initial conditions are

$$u|_{t=0} = u^0,\ v|_{t=0} = v^0,\ r|_{(t=0)} = \sqrt{E_1(u^0,v^0)+C_0}. \tag{3.2}$$

Due to the periodic boundary conditions, we apply the Fourier spectral method for spatial discretization. Taking the two-dimensional (2D) region $\Omega = [0,L_x]\times[0,L_y]$ as an example, we shall introduce the framework of the Fourier spectral method. In our simulations, all spatial functions can be expanded by plane waves. Here, we use $N_x \times N_y$ plane-wave basis functions to discretize the 2D domain. Hence, the space step is defined as $h_x = L_x/N_x$, $h_y = L_y/N_y$. The Fourier approximation space is

$$\mathbb{X}_N = span\{e^{i\alpha_l x}e^{i\beta_p y}| -\frac{N_x}{2} \leq l \leq \frac{N_x}{2}-1, -\frac{N_y}{2} \leq p \leq \frac{N_y}{2}-1\},$$

where $i=\sqrt{-1}$, $\alpha_l = 2\pi l/L_x$, and $\beta_p = 2\pi p/L_y$. Then, we can define the L^2-orthogonal projection operator $\Pi_N : L^2(\Omega) \to \mathbb{X}_N$, which satisfies

$$(\Pi_N\phi - \phi, \Psi) = 0,\ \phi \in L^2(\Omega),\ \forall\ \Psi \in \mathbb{X}_N.$$

The error of the orthogonalization can be estimated: for any $\phi \in H^m_{per}(\Omega)$ and $0 \leq k \leq m$, there exists a constant C such that

$$\|\Pi_N\phi - \phi\|_{H^k} \lesssim h^{m-k}\|\phi\|_{H^m}, \tag{3.3}$$

where $H^m_{per}(\Omega) = \{\phi \in H^m(\Omega)|\phi^{(v)}\ is\ periodic\ on\ \partial\Omega, 0 \leq v \leq m\}$. For simplicity, we consider the case of $L_x = L_y = L$, $N_x = N_y = N$ and $h_x = h_y = h$.

We denote the time step size as $\tau>0$ and $t^n=n\tau$ $(0\le n\le N_T=[T/\tau])$. For any function f, we denote the interpolation as follows:

$$\tilde{f}^n=\frac{3}{2}f^n-\frac{1}{2}f^{n-1},$$
$$\hat{f}^{n+\frac{1}{2}}=\frac{1}{2}(f^n+f^{n+1}),$$

where $f^n=f(t^n)$.

Then, we introduce the fully discrete scheme for the blended model proposed in [22], which combines the SAV approach with the Crank-Nicolson scheme. The second-order fully discrete SAV scheme is as follows. For $n\ge 1$, given u_N^{n-1}, v_N^{n-1} and u_N^n, v_N^n, find u_N^{n+1}, v_N^{n+1} such that

$$\frac{u_N^{n+1}-u_N^n}{M_u\tau}=\Delta\mu_N^{n+\frac{1}{2}}, \tag{3.4}$$
$$\mu_N^{n+\frac{1}{2}}=-\epsilon_u^2\Delta u_N^{n+\frac{1}{2}}+Su_N^{n+\frac{1}{2}}+H(\tilde{u}_N^n,\tilde{v}_N^n)r_N^{n+\frac{1}{2}}, \tag{3.5}$$
$$\frac{v_N^{n+1}-v_N^n}{M_v\tau}=\Delta\xi_N^{n+\frac{1}{2}}-\sigma(v_N^{n+\frac{1}{2}}-\bar{v}_N^{n+\frac{1}{2}}), \tag{3.6}$$
$$\xi_N^{n+\frac{1}{2}}=-\epsilon_v^2\Delta v_N^{n+\frac{1}{2}}+Sv_N^{n+\frac{1}{2}}+G(\tilde{u}_N^n,\tilde{v}_N^n)r_N^{n+\frac{1}{2}}, \tag{3.7}$$
$$r_N^{n+1}-r_N^n=\frac{1}{2}\int_\Omega(H(\tilde{u}_N^n,\tilde{v}_N^n)(u_N^{n+1}-u_N^n)+G(\tilde{u}_N^n,\tilde{v}_N^n)(v_N^{n+1}-v_N^n))d\mathbf{x}. \tag{3.8}$$

The initial value required to apply the second-order scheme is obtained by the following first-order scheme based on the backward Euler method.

$$\frac{u_N^1-u_N^0}{M_u\tau}=\Delta\mu_N^1, \tag{3.9}$$
$$\mu_N^1=-\epsilon_u^2\Delta u_N^1+Su_N^1+H(u_N^0,v_N^0)r_N^1, \tag{3.10}$$
$$\frac{v_N^1-v_N^0}{M_v\tau}=\Delta\xi_N^1-\sigma(v_N^1-\bar{v}_N^1), \tag{3.11}$$
$$\xi_N^1=-\epsilon_v^2\Delta v_N^1+Sv_N^1+G(u_N^0,v_N^0)r_N^1, \tag{3.12}$$
$$r_N^1-r_N^0=\frac{1}{2}\int_\Omega\left[H(u_N^0,v_N^0)(u_N^1-u_N^0)+G(u_N^0,v_N^0)(v_N^1-v_N^0)\right]d\mathbf{x}. \tag{3.13}$$

From the scheme (3.4)-(3.8), we have the mass conservation of numerical solutions

$$\int_\Omega u_N^0 d\mathbf{x}=\int_\Omega u_N^1 d\mathbf{x}=\cdots=\int_\Omega u_N^n d\mathbf{x},$$
$$\int_\Omega v_N^0 d\mathbf{x}=\int_\Omega v_N^1 d\mathbf{x}=\cdots=\int_\Omega v_N^n d\mathbf{x},$$

and the following energy stability [22].

THEOREM 3.1. *Scheme (3.4)-(3.8) has unique solutions u_N^n and v_N^n and satisfies the unconditional energy stability*

$$E_{cn2}^{n+1}-E_{cn2}^n=-\frac{1}{M_u\tau}\left\|u_N^{n+1}-u_N^n\right\|_{-1}-\frac{1}{M_v\tau}\left\|v_N^{n+1}-v_N^n\right\|_{-1}, \tag{3.14}$$

where

$$E_{cn2}^n=\frac{1}{2}(\epsilon_u^2\|\nabla u_N^n\|^2+S\|u_N^n\|^2+\epsilon_v^2\|\nabla v_N^n\|^2+S\|v_N^n\|^2+\sigma\|v_N^n-\bar{v}_N^n\|_{-1}^2)+(r^n)^2-C_0.$$

4. Error estimates for the second-order scheme

In this section, we shall give the error estimates for the fully discrete SAV/CN scheme, as stated in Theorem 4.1. In the proof, the key idea is to obtain the L^∞ boundedness of discrete solutions, which ensures that the derivative of the nonlinear term E_1 can be simplified. To achieve this goal, we first make some preparations. Based on the regularity assumption of exact solutions, we derive the regularity of the scalar auxiliary variable $r(t)$ and the estimates for truncation errors. Then, we utilize mathematical induction and couple the proof of L^∞ boundedness and error estimates in the proof. Finally, we draw the conclusion regarding the error estimates.

We denote the error functions as

$$\begin{cases} e_u^n = u_N^n - u(t^n,x) = u_N^n - \prod_N u(t^n,x) + \prod_N u(t^n,x) - u(t^n,x) \triangleq \ddot{e}_u^n + \breve{e}_u^n, \\ e_v^n = v_N^n - v(t^n,x) = v_N^n - \prod_N v(t^n,x) + \prod_N v(t^n,x) - v(t^n,x) \triangleq \ddot{e}_v^n + \breve{e}_v^n, \\ e_\mu^{n+\frac12} = \mu_N^{n+\frac12} - \prod_N \mu(t^{n+\frac12},x) + \prod_N \mu(t^{n+\frac12},x) - \mu(t^{n+\frac12},x) \triangleq \ddot{e}_\mu^{n+\frac12} + \breve{e}_\mu^{n+\frac12}, \\ e_\xi^{n+\frac12} = \xi_N^{n+\frac12} - \prod_N \xi(t^{n+\frac12},x) + \prod_N \xi(t^{n+\frac12},x) - \xi(t^{n+\frac12},x) \triangleq \ddot{e}_\xi^{n+\frac12} + \breve{e}_\xi^{n+\frac12}, \\ e_r^n = r_N^n - r(t^n). \end{cases}$$

Noting the mass conservation of the system and $1 \in S_N$, we have

$$\bar{e}_u^{n+1} = \bar{e}_u^n = \cdots = \bar{e}_u^0 = \frac{1}{|\Omega|}\int_\Omega u_N^0 - \prod\nolimits_N u(t^0) d\mathbf{x} = \bar{\ddot{e}}_u^0,$$
$$\bar{e}_v^{n+1} = \bar{e}_v^n = \cdots = \bar{e}_v^0 = \frac{1}{|\Omega|}\int_\Omega v_N^0 - \prod\nolimits_N v(t^0) d\mathbf{x} = \bar{\ddot{e}}_v^0.$$

In particular, taking the initial values $u_N^0 = \prod_N u(t^0)$, $v_N^0 = \prod_N v(t^0)$, we obtain

$$\bar{e}_u^n = \bar{\ddot{e}}_u^n = \bar{\ddot{e}}_u^0 = 0, \; \bar{e}_v^n = \bar{\ddot{e}}_v^n = \bar{\ddot{e}}_v^0 = 0.$$

Preparations. Before giving the error estimates, let us make some preparations.

(1) We formulate the Cahn-Hilliard system (3.4)-(3.8) in a truncation form:

$$\frac{u(t^{n+1}) - u(t^n)}{M_u \tau} = \Delta\mu(t^{n+\frac12}) - \frac{1}{M_u\tau} R_u^{n+\frac12}, \tag{4.1}$$

$$\mu(t^{n+\frac12}) = -\epsilon_u^2 \Delta\hat{u}(t^{n+\frac12}) + S\hat{u}(t^{n+\frac12}) + \hat{r}(t^{n+\frac12}) H(\tilde{u}(t^n),\tilde{v}(t^n)) - R_\mu^{n+\frac12}, \tag{4.2}$$

$$\frac{v(t^{n+1}) - v(t^n)}{M_v \tau} = \Delta\xi(t^{n+\frac12}) - \sigma(\hat{v}(t^{n+\frac12}) - \bar{\hat{v}}(t^{n+\frac12})) - \frac{1}{M_v\tau} R_v^{n+\frac12}, \tag{4.3}$$

$$\xi(t^{n+\frac12}) = -\epsilon_v^2 \Delta\hat{v}(t^{n+\frac12}) + S\hat{v}(t^{n+\frac12}) + \hat{r}(t^{n+\frac12}) G(\tilde{u}(t^n),\tilde{v}(t^n)) - R_\xi^{n+\frac12}, \tag{4.4}$$

$$\begin{aligned} r(t^{n+1}) - r(t^n) = \frac12 \int_\Omega \big[& H(\tilde{u}(t^n),\tilde{v}(t^n))(u(t^{n+1}) - u(t^n)) \\ & + G(\tilde{u}(t^n),\tilde{v}(t^n))(v(t^{n+1}) - v(t^n)) \big] d\mathbf{x} - R_r^{n+\frac12}, \end{aligned} \tag{4.5}$$

where

$$\begin{aligned} R_u^{n+\frac12} &= u_t(t^{n+\frac12})\tau - u(t^{n+1}) + u(t^n), \\ R_\mu^{n+\frac12} &= \epsilon_u^2 \Delta(u(t^{n+\frac12}) - \hat{u}(t^{n+\frac12})) - S(u(t^{n+\frac12}) - \hat{u}(t^{n+\frac12})) \\ &\quad + \hat{r}(t^{n+\frac12}) H(\tilde{u}(t^n),\tilde{v}(t^n)) - r(t^{n+\frac12}) H(u(t^{n+\frac12}), v(t^{n+\frac12})), \\ R_v^{n+\frac12} &= v_t(t^{n+\frac12})\tau - v(t^{n+1}) + v(t^n) + M_v\tau\sigma(v(t^{n+\frac12}) - \hat{v}(t^{n+\frac12})), \end{aligned}$$

$$\begin{aligned}
R_{\xi}^{n+\frac{1}{2}} =& \epsilon_v^2\Delta(v(t^{n+\frac{1}{2}})-\hat{v}(t^{n+\frac{1}{2}}))-S(v(t^{n+\frac{1}{2}})-\hat{v}(t^{n+\frac{1}{2}}))\\
&+\hat{r}(t^{n+\frac{1}{2}})G(\tilde{u}(t^n),\tilde{v}(t^n))-r(t^{n+\frac{1}{2}})G(u(t^{n+\frac{1}{2}}),v(t^{n+\frac{1}{2}})),\\
R_r^{n+\frac{1}{2}} =& r_t(t^{n+\frac{1}{2}})\tau-r(t^{n+1})+r(t^n)\\
&+\frac{1}{2}\int_\Omega H(u(t^{n+\frac{1}{2}}),v(t^{n+\frac{1}{2}}))(u(t^{n+1})-u(t^n)-u_t(t^{n+\frac{1}{2}})\tau)d\mathbf{x}\\
&-\frac{1}{2}\int_\Omega (H(u(t^{n+\frac{1}{2}}),v(t^{n+\frac{1}{2}}))-H(\tilde{u}(t^n),\tilde{v}(t^n)))(u(t^{n+1})-u(t^n))d\mathbf{x}\\
&+\frac{1}{2}\int_\Omega G(u(t^{n+\frac{1}{2}}),v(t^{n+\frac{1}{2}}))(v(t^{n+1})-v(t^n)-v_t(t^{n+\frac{1}{2}})\tau)d\mathbf{x}\\
&-\frac{1}{2}\int_\Omega (G(u(t^{n+\frac{1}{2}}),v(t^{n+\frac{1}{2}}))-G(\tilde{u}(t^n),\tilde{v}(t^n)))(v(t^{n+1})-v(t^n))d\mathbf{x}.
\end{aligned}$$

(2) Theorem 3.1 has implied the boundedness of functions u_N^k, v_N^k and r_N^k as follows:

$$max\left\{\left\|u_N^k\right\|_{H^1},\left\|v_N^k\right\|_{H^1},\left\|r_N^k\right\|_{H^1}\right\}\leq C,\quad k\leq T_{max}/\tau,$$

where C is a constant depending on the domain and initial data.
We assume that the exact solutions u,v,r of the system (2.3)-(2.4) possess the following regularity conditions:

$$\begin{cases}
u,v\in L^\infty(0,T;H_{per}^{m+1}),\\
u_t,v_t\in L^\infty(0,T;H_{per}^{-1})\cap L^\infty(0,T;H_{per}^1),\\
u_{tt},v_{tt}\in L^\infty(0,T;L_{per}^2)\cap L^2(0,T;H_{per}^3),v_{tt}\in L^2(0,T;H_{per}^{-1}),\\
u_{ttt},v_{ttt}\in L^2(0,T;L^2)\cap L^2(0,T;H_{per}^{-1}),\\
\|\nabla u\|_{L^\infty((0,T)\times\Omega)},\|\nabla v\|_{L^\infty((0,T)\times\Omega)}\leq C.
\end{cases}\tag{4.6}$$

Based on the regularity assumption of exact solutions, we can derive the regularity of the scalar auxiliary variable $r(t)$.

LEMMA 4.1. *Under the regularity conditions (4.6), we have r_{tt}, $r_{ttt}\in L^2(0,T)$.*

Proof. Applying Hölder inequality, Sobolev embedding theorem and chain rule, the proof is straightforward. Here, we give the detailed proof of the lemma in Appendix A. □

One can now easily establish the following estimates for truncation errors.

LEMMA 4.2. *Under the regularity conditions (4.6), the truncation errors satisfy*

$$\left\|R_u^{n+\frac{1}{2}}\right\|_{-1}^2\lesssim\tau^5\int_{t^n}^{t^{n+1}}\|u_{ttt}\|_{-1}^2ds,\tag{4.7}$$

$$\left\|R_v^{n+\frac{1}{2}}\right\|_{-1}^2\lesssim\tau^5\int_{t^n}^{t^{n+1}}\left(\|v_{tt}\|_{-1}^2+\|v_{ttt}\|_{-1}^2\right)ds,\tag{4.8}$$

$$\left\|\nabla R_\mu^{n+\frac{1}{2}}\right\|^2\lesssim\tau^3\int_{t^{n-1}}^{t^{n+1}}\left(\|u_{tt}\|_{H^1}^2+\|v_{tt}\|_{H^1}^2+\|u_{tt}\|_{H^3}^2+|r_{tt}|^2\right)ds,\tag{4.9}$$

$$\left\|\nabla R_\xi^{n+\frac{1}{2}}\right\|^2\lesssim\tau^3\int_{t^{n-1}}^{t^{n+1}}\left(\|u_{tt}\|_{H^1}^2+\|v_{tt}\|_{H^1}^2+\|v_{tt}\|_{H^3}^2+|r_{tt}|^2\right)ds,\tag{4.10}$$

$$|R_r^{n+\frac{1}{2}}|^2\lesssim\tau^5\int_{t^{n-1}}^{t^{n+1}}\left(\|u_{tt}\|_{H^1}^2+\|v_{tt}\|_{H^1}^2+\|u_{ttt}\|^2+\|v_{ttt}\|^2+|r_{ttt}|^2\right)ds.\tag{4.11}$$

Proof. Note that

$$f(t^{n+1})-f(t^n)-f_t(t^{n+1})\tau \lesssim \tau^2,$$
$$|\frac{1}{2}(f(t^{n+1})+f(t^{n-1}))-f(t^n)|^2 \lesssim \tau^3 \int_{t^{n-1}}^{t^{n+1}} |\frac{\partial^2 f}{\partial t^2}|^2 ds,$$

the proof of this lemma is simple. The detailed proof of the lemma is given in Appendix B. ∎

(3) Subtracting (3.4)-(3.8) from (4.1)-(4.5), we can derive the error equations as

$$(\ddot{e}_u^{n+1}-\ddot{e}_u^n,q)+M_u\tau(\nabla\ddot{e}_\mu^{n+\frac{1}{2}},\nabla q)=(R_u^{n+\frac{1}{2}},q), \tag{4.12}$$

$$\begin{aligned}(\ddot{e}_\mu^{n+\frac{1}{2}},\Psi)=&\epsilon_u^2(\nabla\hat{\ddot{e}}_u^{n+\frac{1}{2}},\nabla\Psi)+S(\hat{\ddot{e}}_u^{n+\frac{1}{2}},\Psi)+r_N^{n+\frac{1}{2}}(H(\tilde{u}_N^n,\tilde{v}_N^n),\Psi)\\ &-\hat{r}(t^{n+\frac{1}{2}})(H(\tilde{u}(t^n),\tilde{v}(t^n)),\Psi)+(R_\mu^{n+\frac{1}{2}},\Psi),\end{aligned} \tag{4.13}$$

$$(\ddot{e}_v^{n+1}-\ddot{e}_v^n,q^*)+M_v\tau(\nabla\ddot{e}_\xi^{n+\frac{1}{2}},\nabla q^*)=-M_v\tau\sigma(\hat{\ddot{e}}_v^{n+\frac{1}{2}}-\bar{\hat{\ddot{e}}}_v^{n+\frac{1}{2}},q^*)+(R_v^{n+\frac{1}{2}},q^*), \tag{4.14}$$

$$\begin{aligned}(\ddot{e}_\xi^{n+\frac{1}{2}},\Psi^*)=&\epsilon_v^2(\nabla\hat{\ddot{e}}_v^{n+\frac{1}{2}},\nabla\Psi^*)+S(\hat{\ddot{e}}_v^{n+\frac{1}{2}},\Psi^*)+r_N^{n+\frac{1}{2}}(G(\tilde{u}_N^n,\tilde{v}_N^n),\Psi^*)\\ &-\hat{r}(t^{n+\frac{1}{2}})(G(\tilde{u}(t^n),\tilde{v}(t^n)),\Psi^*)+(R_\xi^{n+\frac{1}{2}},\Psi^*),\end{aligned} \tag{4.15}$$

$$\begin{aligned}e_r^{n+1}-e_r^n=&\frac{1}{2}\int_\Omega (H(\tilde{u}_N^n,\tilde{v}_N^n)(u_N^{n+1}-u_N^n)-H(\tilde{u}(t^n),\tilde{v}(t^n))(u(t^{n+1})-u(t^n))\\ &+G(\tilde{u}_N^n,\tilde{v}_N^n)(v_N^{n+1}-v_N^n)-G(\tilde{u}(t^n),\tilde{v}(t^n))(v(t^{n+1})-v(t^n)))d\mathbf{x}\\ &+R_r^{n+\frac{1}{2}},\end{aligned} \tag{4.16}$$

where q, Ψ, q^*, and $\Psi^*\in\mathbb{X}_N$.

We now establish the error estimates for scheme (3.4)-(3.8). The main result concerning the error estimate can be derived if we can complete the proof of the following lemma.

Lemma 4.3. *Supposing that the exact solutions of the system satisfy the regularity assumption (4.6). Then there exist two positive constants τ_0 and h_0 such that, for any $\tau<\tau_0$ and $h<h_0$, the solutions u_N^n and v_N^n of (3.4)-(3.8) satisfy*

$$max\{\|u_N^n\|_{L^\infty},\|v_N^n\|_{L^\infty}\}\le C=\max_{0\leqslant t\leqslant T_{max}}\{\|u(t)\|_{L^\infty},\|v(t)\|_{L^\infty}\}+2, \tag{4.17}$$

where $n=0,1,2,\cdots,[T_{max}/\tau]$.

Proof. Taking the proof of the L^∞ boundedness of v_N^n as an example, we apply mathematical induction to prove this lemma. When $n=0$, using the Sobolev embedding theorem, we have

$$\begin{aligned}\|v_N^0\|_{L^\infty}&=\|\Pi_N v^0\|_{L^\infty}\leqslant\|\Pi_N v^0-v^0\|_{L^\infty}+\|v^0\|_{L^\infty}\\ &\lesssim\|\Pi_N v^0-v^0\|_{H^1}+\|v^0\|_{L^\infty}\\ &\leqslant C_1h^{m-1}\|v^0\|_{H^m}+\|v^0\|_{L^\infty}\leqslant C, for\ d=2,\\ \|v_N^0\|_{L^\infty}&\lesssim\|\Pi_N v^0-v^0\|_{H^2}+\|v^0\|_{L^\infty}\\ &\leqslant C_1h^{m-2}\|v^0\|_{H^m}+\|v^0\|_{L^\infty}\leqslant C, for\ d=3,\end{aligned}$$

where $h \leqslant h_1 = min\{ \sqrt[m-1]{2/(C_1\|v^0\|_{H^m})}, \sqrt[m-2]{2/(C_1\|v^0\|_{H^m})}\}$. Supposing that $\|v_N^n\|_{L^\infty} \leqslant C$ is valid for $n=0,1,2,\cdots,k$, we shall prove that $\|v_N^{k+1}\|_{L^\infty} \leqslant C$ is also valid in the following four steps.

Step 1. Taking $q=\ddot{e}_\mu^{n+\frac{1}{2}}$, $\Psi=\ddot{e}_u^{n+1}-\ddot{e}_u^n$, $q^*=\ddot{e}_\xi^{n+\frac{1}{2}}$, $\Psi^*=\ddot{e}_v^{n+1}-\ddot{e}_v^n$ in (4.12)-(4.15) and multiplying (4.16) by $e_r^{n+1}+e_r^n$, we derive

$$(\ddot{e}_u^{n+1}-\ddot{e}_u^n,\ddot{e}_\mu^{n+\frac{1}{2}})+M_u\tau\left\|\nabla\ddot{e}_\mu^{n+\frac{1}{2}}\right\|^2=(R_u^{n+\frac{1}{2}},\ddot{e}_\mu^{n+\frac{1}{2}}), \tag{4.18}$$

$$\begin{aligned}(\ddot{e}_\mu^{n+\frac{1}{2}},\ddot{e}_u^{n+1}-\ddot{e}_u^n)=&\frac{\epsilon_u^2}{2}(\|\nabla\ddot{e}_u^{n+1}\|^2-\|\nabla\ddot{e}_u^n\|^2)+\frac{S}{2}(\|\ddot{e}_u^{n+1}\|^2-\|\ddot{e}_u^n\|^2)\\&+r_N^{n+\frac{1}{2}}(H(\tilde{u}_N^n,\tilde{v}_N^n),\ddot{e}_u^{n+1}-\ddot{e}_u^n)-\hat{r}(t^{n+\frac{1}{2}})(H(\tilde{u}(t^n),\tilde{v}(t^n)),\ddot{e}_u^{n+1}-\ddot{e}_u^n)\\&+(R_\mu^{n+\frac{1}{2}},\ddot{e}_u^{n+1}-\ddot{e}_u^n),\end{aligned} \tag{4.19}$$

$$(\ddot{e}_v^{n+1}-\ddot{e}_v^n,\ddot{e}_\xi^{n+\frac{1}{2}})+M_v\tau\left\|\nabla\ddot{e}_\xi^{n+\frac{1}{2}}\right\|^2=-M_v\tau\sigma(\hat{\ddot{e}}_v^{n+\frac{1}{2}}-\bar{\ddot{e}}_v^{n+\frac{1}{2}},\ddot{e}_\xi^{n+\frac{1}{2}})+(R_v^{n+\frac{1}{2}},\ddot{e}_\xi^{n+\frac{1}{2}}), \tag{4.20}$$

$$\begin{aligned}(\ddot{e}_\xi^{n+\frac{1}{2}},\ddot{e}_v^{n+1}-\ddot{e}_v^n)=&\frac{\epsilon_v^2}{2}(\|\nabla\ddot{e}_v^{n+1}\|^2-\|\nabla\ddot{e}_v^n\|^2)+\frac{S}{2}(\|\ddot{e}_v^{n+1}\|^2-\|\ddot{e}_v^n\|^2)\\&+r_N^{n+\frac{1}{2}}(G(\tilde{u}_N^n,\tilde{v}_N^n),\ddot{e}_v^{n+1}-\ddot{e}_v^n)-\hat{r}(t^{n+\frac{1}{2}})(G(\tilde{u}(t^n),\tilde{v}(t^n)),\ddot{e}_v^{n+1}-\ddot{e}_v^n)\\&+(R_\xi^{n+\frac{1}{2}},\ddot{e}_v^{n+1}-\ddot{e}_v^n),\end{aligned} \tag{4.21}$$

$$\begin{aligned}(e_r^{n+1})^2-(e_r^n)^2=&\hat{e}_r^{n+\frac{1}{2}}\int_\Omega(H(\tilde{u}_N^n,\tilde{v}_N^n)(u_N^{n+1}-u_N^n)-H(\tilde{u}(t^n),\tilde{v}(t^n))(u(t^{n+1})-u(t^n))\\&+G(\tilde{u}_N^n,\tilde{v}_N^n)(v_N^{n+1}-v_N^n)-G(\tilde{u}(t^n),\tilde{v}(t^n))(v(t^{n+1})-v(t^n)))d\mathbf{x}\\&+2(R_r^{n+\frac{1}{2}},\hat{e}_r^{n+\frac{1}{2}}).\end{aligned} \tag{4.22}$$

Combining (4.18)-(4.22), we obtain

$$\begin{aligned}&\frac{\epsilon_u^2}{2}(\|\nabla\ddot{e}_u^{n+1}\|^2-\|\nabla\ddot{e}_u^n\|^2)+\frac{S}{2}(\|\ddot{e}_u^{n+1}\|^2-\|\ddot{e}_u^n\|^2)+M_u\tau\left\|\nabla\ddot{e}_\mu^{n+\frac{1}{2}}\right\|^2+(e_r^{n+1})^2\\&\quad+\frac{\epsilon_v^2}{2}(\|\nabla\ddot{e}_v^{n+1}\|^2-\|\nabla\ddot{e}_v^n\|^2)+\frac{S}{2}(\|\ddot{e}_v^{n+1}\|^2-\|\ddot{e}_v^n\|^2)+M_v\tau\left\|\nabla\ddot{e}_\xi^{n+\frac{1}{2}}\right\|^2-(e_r^n)^2\\&=\sum_{i=1}^4 Q_i,\end{aligned} \tag{4.23}$$

with

$$Q_1=(R_u^{n+\frac{1}{2}},\ddot{e}_\mu^{n+\frac{1}{2}})-(R_\mu^{n+\frac{1}{2}},\ddot{e}_u^{n+1}-\ddot{e}_u^n)+(R_v^{n+\frac{1}{2}},\ddot{e}_\xi^{n+\frac{1}{2}}),$$

$$Q_2=-M_v\tau\sigma(\hat{\ddot{e}}_v^{n+\frac{1}{2}}-\bar{\ddot{e}}_v^{n+\frac{1}{2}},\ddot{e}_\xi^{n+\frac{1}{2}})-(R_\xi^{n+\frac{1}{2}},\ddot{e}_v^{n+1}-\ddot{e}_v^n),$$

$$\begin{aligned}Q_3=&-r_N^{n+\frac{1}{2}}(H(\tilde{u}_N^n,\tilde{v}_N^n),\ddot{e}_u^{n+1}-\ddot{e}_u^n)+\hat{r}(t^{n+\frac{1}{2}})(H(\tilde{u}(t^n),\tilde{v}(t^n)),\ddot{e}_u^{n+1}-\ddot{e}_u^n)\\&-r_N^{n+\frac{1}{2}}(G(\tilde{u}_N^n,\tilde{v}_N^n),\ddot{e}_v^{n+1}-\ddot{e}_v^n)+\hat{r}(t^{n+\frac{1}{2}})(G(\tilde{u}(t^n),\tilde{v}(t^n)),\ddot{e}_v^{n+1}-\ddot{e}_v^n),\end{aligned}$$

and Q_4 being the right-hand side of (4.22).

Step 2. Below, we shall give an analysis for each term on the right-hand side of (4.23). First, noting the regularity assumption (4.6) and using (4.12), we have

$$
\begin{aligned}
Q_1 &= (R_u^{n+\frac{1}{2}}, \ddot{e}_\mu^{n+\frac{1}{2}}) + (R_v^{n+\frac{1}{2}}, \ddot{e}_\xi^{n+\frac{1}{2}}) - (R_\mu^{n+\frac{1}{2}}, M_u\tau\Delta\ddot{e}_\mu^{n+\frac{1}{2}} + R_u^{n+\frac{1}{2}}) \\
&\le \frac{1}{6}M_u\tau\left\|\nabla\ddot{e}_\mu^{n+\frac{1}{2}}\right\|^2 + \frac{C}{\tau}\left\|R_u^{n+\frac{1}{2}}\right\|_{-1}^2 + \frac{1}{12}M_v\tau\left\|\nabla\ddot{e}_\xi^{n+\frac{1}{2}}\right\|^2 + \frac{C}{\tau}\left\|R_v^{n+\frac{1}{2}}\right\|_{-1}^2 \\
&\quad + C\tau\left\|\nabla R_\mu^{n+\frac{1}{2}}\right\|^2. \qquad (4.24)
\end{aligned}
$$

Second, we give an estimate for Q_2, in which the first term is directly caused by the nonlocal term. By using (4.15), the mass conservation of e_v and given that $(\ddot{e}_v - \bar{\ddot{e}}_v) \in L_0^2(\Omega)$, we obtain

$$
\begin{aligned}
Q_2 &= -\frac{1}{2}M_v\tau\sigma(\ddot{e}_v^{n+1} - \bar{\ddot{e}}_v^{n+1}, \ddot{e}_\xi^{n+\frac{1}{2}}) - \frac{1}{2}M_v\tau\sigma(\ddot{e}_v^{n} - \bar{\ddot{e}}_v^{n}, \ddot{e}_\xi^{n+\frac{1}{2}}) \\
&\qquad - (R_\xi^{n+\frac{1}{2}}, M_v\tau\Delta\ddot{e}_\xi^{n+\frac{1}{2}} - M_v\tau\sigma(\hat{\ddot{e}}_v^{n+\frac{1}{2}} - \bar{\hat{\ddot{e}}}_v^{n+\frac{1}{2}}) + R_v^{n+\frac{1}{2}}) \\
&\le \frac{1}{6}M_v\tau\left\|\nabla\ddot{e}_\xi^{n+\frac{1}{2}}\right\|^2 + C\tau\left\|\nabla R_\xi^{n+\frac{1}{2}}\right\|^2 + \frac{C}{\tau}\left\|R_v^{n+\frac{1}{2}}\right\|_{-1}^2 \\
&\qquad + C\tau(\left\|\ddot{e}_v^{n+1} - \bar{\ddot{e}}_v^{n+1}\right\|_{-1}^2 + \|\ddot{e}_v^{n} - \bar{\ddot{e}}_v^{n}\|_{-1}^2). \qquad (4.25)
\end{aligned}
$$

To complete the estimation of Q_2, it is necessary to estimate $\|\ddot{e}_v^{n} - \bar{\ddot{e}}_v^{n}\|_{-1}^2$. Thus, we take $q^* = (-\Delta)^{-1}(\ddot{e}_v^{n+1} - \ddot{e}_v^{n})$ in (4.21) and have

$$
\begin{aligned}
&\left\|\ddot{e}_v^{n+1} - \bar{\ddot{e}}_v^{n+1}\right\|_{-1}^2 - \|\ddot{e}_v^{n} - \bar{\ddot{e}}_v^{n}\|_{-1}^2 \le \left\|\ddot{e}_v^{n+1} - \ddot{e}_v^{n}\right\|_{-1}^2 \\
&= (M_v\tau\Delta\ddot{e}_\xi^{n+\frac{1}{2}} - M_v\tau\sigma(\hat{\ddot{e}}_v^{n+\frac{1}{2}} - \bar{\hat{\ddot{e}}}_v^{n+\frac{1}{2}}) + R_v^{n+\frac{1}{2}}, (-\Delta)^{-1}(\ddot{e}_v^{n+1} - \ddot{e}_v^{n})) \\
&\le C\tau\left\|\ddot{e}_v^{n+1} - \ddot{e}_v^{n}\right\|_{-1}^2 + \frac{1}{12}M_v\tau\left\|\nabla\ddot{e}_\xi^{n+1}\right\|^2 + \frac{C}{\tau}\left\|R_v^{n+\frac{1}{2}}\right\|_{-1}^2 \\
&\qquad + C\tau(\left\|\ddot{e}_v^{n+1} - \bar{\ddot{e}}_v^{n+1}\right\|_{-1}^2 - \|\ddot{e}_v^{n} - \bar{\ddot{e}}_v^{n}\|_{-1}^2) \\
&\le \frac{1}{12}M_v\tau\left\|\nabla\ddot{e}_\xi^{n+1}\right\|^2 + \frac{C}{\tau}\left\|R_v^{n+\frac{1}{2}}\right\|_{-1}^2 + C\tau(\left\|\ddot{e}_v^{n+1} - \bar{\ddot{e}}_v^{n+1}\right\|_{-1}^2 + \|\ddot{e}_v^{n} - \bar{\ddot{e}}_v^{n}\|_{-1}^2). \qquad (4.26)
\end{aligned}
$$

Combining (4.26) with (4.25), one can estimate Q_2.

Third, the third term on the right-hand side of (4.23) can be transformed into

$$
\begin{aligned}
Q_3 &= -\hat{e}_r^{n+\frac{1}{2}}(H(\tilde{u}_N^n, \tilde{v}_N^n), \ddot{e}_u^{n+1} - \ddot{e}_u^{n}) - \hat{r}(t^{n+\frac{1}{2}})(H(\tilde{u}_N^n, \tilde{v}_N^n) - H(\tilde{u}(t^n), \tilde{v}(t^n)), \ddot{e}_u^{n+1} - \ddot{e}_u^{n}) \\
&\quad - \hat{e}_r^{n+\frac{1}{2}}(G(\tilde{u}_N^n, \tilde{v}_N^n), \ddot{e}_v^{n+1} - \ddot{e}_v^{n}) - \hat{r}(t^{n+\frac{1}{2}})(G(\tilde{u}_N^n, \tilde{v}_N^n) - G(\tilde{u}(t^n), \tilde{v}(t^n)), \ddot{e}_v^{n+1} - \ddot{e}_v^{n}) \\
&\le -\hat{e}_r^{n+\frac{1}{2}}(H(\tilde{u}_N^n, \tilde{v}_N^n), \ddot{e}_u^{n+1} - \ddot{e}_u^{n}) - \hat{e}_r^{n+\frac{1}{2}}(G(\tilde{u}_N^n, \tilde{v}_N^n), \ddot{e}_v^{n+1} - \ddot{e}_v^{n}) \\
&\quad + \frac{1}{12}M_u\tau\left\|\nabla\ddot{e}_\mu^{n+\frac{1}{2}}\right\|^2 + \frac{C}{\tau}\left\|R_u^{n+\frac{1}{2}}\right\|_{-1}^2 + C\tau\|\nabla H(\tilde{u}_N^n, \tilde{v}_N^n) - \nabla H(\tilde{u}(t^n), \tilde{v}(t^n))\|^2 \\
&\quad + \frac{1}{12}M_v\tau\left\|\nabla\ddot{e}_\xi^{n+\frac{1}{2}}\right\|^2 + \frac{C}{\tau}\left\|R_v^{n+\frac{1}{2}}\right\|_{-1}^2 + C\tau\left\|\hat{\ddot{e}}_v^{n+\frac{1}{2}} - \bar{\hat{\ddot{e}}}_v^{n+\frac{1}{2}}\right\|_{-1}^2 \\
&\quad + C\tau\|\nabla G(\tilde{u}_N^n, \tilde{v}_N^n) - \nabla G(\tilde{u}(t^n), \tilde{v}(t^n))\|^2. \qquad (4.27)
\end{aligned}
$$

The fifth and last term on the right-hand side of (4.27) can be estimated in a similar way. Below, we take the proof of the fifth term as an example. Since we have

$$\begin{aligned}\nabla H(\tilde{u}_N^n,\tilde{v}_N^n)-\nabla H(\tilde{u}(t^n),\tilde{v}(t^n))&=\frac{\nabla f(\tilde{u}_N^n,\tilde{v}_N^n)}{\sqrt{E_1(\tilde{u}_N^n,\tilde{v}_N^n)+C_0}}-\frac{\nabla f(\tilde{u}(t^n),\tilde{v}(t^n))}{\sqrt{E_1(\tilde{u}(t^n),\tilde{v}(t^n))+C_0}}\\ =\frac{\nabla f(\tilde{u}_N^n,\tilde{v}_N^n)-\nabla f(\tilde{u}(t^n),\tilde{v}(t^n))}{\sqrt{E_1(\tilde{u}_N^n,\tilde{v}_N^n)+C_0}}&\\ -\nabla f(\tilde{u}(t^n),\tilde{v}(t^n))\left(\frac{1}{\sqrt{E_1(\tilde{u}(t^n),\tilde{v}(t^n))+C_0}}-\frac{1}{\sqrt{E_1(\tilde{u}_N^n,\tilde{v}_N^n)+C_0}}\right)&\triangleq A_1+A_2,\end{aligned} \tag{4.28}$$

For the first term on the right-hand side of (4.28), we have the following estimate:

$$\begin{aligned}\|A_1\|^2&\lesssim\|\nabla f(\tilde{u}_N^n,\tilde{v}_N^n)-\nabla f(\tilde{u}(t^n),\tilde{v}(t^n))\|^2\\ &\lesssim\|\nabla f(\tilde{u}_N^n,\tilde{v}_N^n)-\nabla f(\tilde{u}(t^n),\tilde{v}_N^n)\|^2+\|\nabla f(\tilde{u}(t^n),\tilde{v}_N^n)-\nabla f(\tilde{u}(t^n),\tilde{v}(t^n))\|^2\\ &\lesssim\|f_u(\tilde{u}_N^n,\tilde{v}_N^n)\nabla\tilde{u}_N^n-f_u(\tilde{u}(t^n),\tilde{v}_N^n)\nabla\tilde{u}(t^n)\|^2\\ &\quad+\|f_v(\tilde{u}_N^n,\tilde{v}_N^n)\nabla\tilde{v}_N^n-f_v(\tilde{u}(t^n),\tilde{v}_N^n)\nabla\tilde{v}_N^n\|^2\\ &\quad\|f_u(\tilde{u}(t^n),\tilde{v}_N^n)\nabla\tilde{u}(t^n)-f_u(\tilde{u}(t^n),\tilde{v}(t^n))\nabla\tilde{u}(t^n)\|^2\\ &\quad+\|f_v(\tilde{u}(t^n),\tilde{v}_N^n)\nabla\tilde{v}_N^n-f_v(\tilde{u}(t^n),\tilde{v}(t^n))\nabla\tilde{v}(t^n)\|^2\triangleq\sum_{i=1}^4 B_i.\end{aligned} \tag{4.29}$$

Using Hölder inequality and Soblev embedding, the first two terms on the right-hand side of (4.29) can be estimated by

$$\begin{aligned}B_1&\le\|f_u(\tilde{u}_N^n,\tilde{v}_N^n)\nabla\tilde{e}_u^n\|^2+\|(f_u(\tilde{u}_N^n,\tilde{v}_N^n)-f_u(\tilde{u}(t^n),\tilde{v}_N^n))\nabla\tilde{u}(t^n)\|^2\\ &=\|f_{uu}(\xi^*,\tilde{v}_N^n)(\tilde{u}_N^n-\tilde{u}(t^n))\nabla\tilde{u}(t^n)\|^2+\|f_u(\tilde{u}_N^n,\tilde{v}_N^n)\nabla\tilde{e}_u^n\|^2\\ &\lesssim\|(\tilde{u}_N^n-\tilde{u}(t^n))\nabla\tilde{u}(t^n)\|^2+\|\nabla\tilde{e}_u^n\|^2\\ &\lesssim\|\tilde{u}_N^n-\tilde{u}(t^n)\|_{L^3}^2\|\nabla\tilde{u}(t^n)\|_{L^6}^2+\|\nabla\tilde{e}_u^n\|^2\\ &\lesssim\|\tilde{u}_N^n-\tilde{u}(t^n)\|_{H^1}^2\|\tilde{u}(t^n)\|_{H^2}^2+\|\nabla\tilde{e}_u^n\|^2\\ &\lesssim\|\tilde{e}_u^n\|^2+\|\nabla\tilde{e}_u^n\|^2,\end{aligned}$$

and

$$B_2=\|f_{uv}(\xi^*,\tilde{v}_N^n)(\tilde{u}_N^n-\tilde{u}(t^n))\nabla\tilde{v}_N^n\|^2\lesssim\|\tilde{e}_u^n\|_{H^1}^2. \tag{4.30}$$

The latter two items can be handled in a similar way. Then, we obtain

$$\|A_1\|^2\lesssim\|\tilde{e}_u^n\|^2+\|\nabla\tilde{e}_u^n\|^2+\|\tilde{e}_v^n\|^2+\|\nabla\tilde{e}_v^n\|^2, \tag{4.31}$$

and

$$\|A_2\|^2\lesssim\|E_1(\tilde{u}_N^n,\tilde{v}_N^n)-E_1(\tilde{u}(t^n),\tilde{v}(t^n))\|^2\lesssim\|\tilde{e}_u^n\|^2+\|\tilde{e}_v^n\|^2. \tag{4.32}$$

Combining (4.28), (4.31) and (4.32), we derive

$$\|\nabla H(\tilde{u}_N^n,\tilde{v}_N^n)-\nabla H(\tilde{u}(t^n),\tilde{v}(t^n))\|^2\lesssim\|\tilde{e}_u^n\|^2+\|\nabla\tilde{e}_u^n\|^2+\|\tilde{e}_v^n\|^2+\|\nabla\tilde{e}_v^n\|^2. \tag{4.33}$$

Similarly, the last term on the right-hand side of (4.28) can be controlled by

$$\|\nabla G(\tilde{u}_N^n,\tilde{v}_N^n)-\nabla G(\tilde{u}(t^n),\tilde{v}(t^n))\|^2 \lesssim \|\tilde{e}_u^n\|^2+\|\nabla\tilde{e}_u^n\|^2+\|\tilde{e}_v^n\|^2+\|\nabla\tilde{e}_v^n\|^2. \tag{4.34}$$

Using (4.27), (4.33) and (4.34), we can derive the estimate of Q_3.

Finally, for the first and second terms in Q_4, we have

$$\begin{aligned}
&\hat{e}_r^{n+\frac{1}{2}}\int_\Omega (H(\tilde{u}_N^n,\tilde{v}_N^n)(u_N^{n+1}-u_N^n)-H(\tilde{u}(t^n),\tilde{v}(t^n))(u(t^{n+1})-u(t^n))d\mathbf{x}\\
&=\hat{e}_r^{n+\frac{1}{2}}(H(\tilde{u}_N^n,\tilde{v}_N^n),e_u^{n+1}-e_u^n)+\hat{e}_r^{n+\frac{1}{2}}(H(\tilde{u}_N^n,\tilde{v}_N^n)-H(\tilde{u}(t^n),\tilde{v}(t^n)),u(t^{n+1})-u(t^n))\\
&\leq \hat{e}_r^{n+\frac{1}{2}}(H(\tilde{u}_N^n,\tilde{v}_N^n),e_u^{n+1}-e_u^n)\\
&\quad +C\tau\|u_t\|_{L^\infty(0,T;H^{-1})}((e_r^{n+1})^2+(e_r^n)^2+\|\nabla H(\tilde{u}_N^n,\tilde{v}_N^n)-\nabla H(\tilde{u}(t^n),\tilde{v}(t^n))\|^2),
\end{aligned} \tag{4.35}$$

and

$$\begin{aligned}
&\hat{e}_r^{n+\frac{1}{2}}\int_\Omega (G(\tilde{u}_N^n,\tilde{v}_N^n)(v_N^{n+1}-v_N^n)-G(\tilde{u}(t^n),\tilde{v}(t^n))(v(t^{n+1})-v(t^n))d\mathbf{x}\\
&\leq \hat{e}_r^{n+\frac{1}{2}}(G(\tilde{u}_N^n,\tilde{v}_N^n),e_v^{n+1}-e_v^n)\\
&\quad +C\tau\|v_t\|_{L^\infty(0,T;H^{-1})}((e_r^{n+1})^2+(e_r^n)^2+\|\nabla G(\tilde{u}_N^n,\tilde{v}_N^n)-\nabla G(\tilde{u}(t^n),\tilde{v}(t^n))\|^2).
\end{aligned} \tag{4.36}$$

The last term in Q_4 can be controlled by:

$$2(R_r^{n+\frac{1}{2}},\hat{e}_r^{n+\frac{1}{2}})\leq C\tau(\hat{e}_r^{n+\frac{1}{2}})^2+\frac{C}{\tau}|R_r^{n+\frac{1}{2}}|^2. \tag{4.37}$$

Noting (4.33)-(4.37), and Lemma 4.2, Q_4 can be estimated by

$$\begin{aligned}
Q_4\leq&\,\hat{e}_r^{n+\frac{1}{2}}(H(\tilde{u}_N^n,\tilde{v}_N^n),e_u^{n+1}-e_u^n)+\hat{e}_r^{n+\frac{1}{2}}(G(\tilde{u}_N^n,\tilde{v}_N^n),e_v^{n+1}-e_v^n)\\
&+C\tau((e_r^{n+1})^2+(e_r^n)^2+\|\tilde{e}_u^n\|^2+\|\nabla\tilde{e}_u^n\|^2+\|\tilde{e}_v^n\|^2+\|\nabla\tilde{e}_v^n\|^2).
\end{aligned} \tag{4.38}$$

Step 3. Based on the above estimates (3.3), (4.23)-(4.27), (4.33), (4.34), (4.38) and Lemma 4.2, we have

$$\begin{aligned}
&\frac{\epsilon_u^2}{2}(\|\nabla\ddot{e}_u^{n+1}\|^2-\|\nabla\ddot{e}_u^n\|^2)+\frac{S}{2}(\|\ddot{e}_u^{n+1}\|^2-\|\ddot{e}_u^n\|^2)+M_u\tau\left\|\nabla\ddot{e}_\mu^{n+\frac{1}{2}}\right\|^2+\frac{\epsilon_v^2}{2}(\|\nabla\ddot{e}_v^{n+1}\|^2-\|\nabla\ddot{e}_v^n\|^2)\\
&\quad+\frac{S}{2}(\|\ddot{e}_v^{n+1}\|^2-\|\ddot{e}_v^n\|^2)+M_v\tau\left\|\nabla\ddot{e}_\xi^{n+\frac{1}{2}}\right\|^2+(e_r^{n+1})^2-(e_r^n)^2+\|\ddot{e}_v^{n+1}-\bar{\ddot{e}}_v^{n+1}\|_{-1}^2-\|\ddot{e}_v^n-\bar{\ddot{e}}_v^n\|_{-1}^2\\
&\leq\frac{1}{4}M_u\tau\left\|\nabla\ddot{e}_\mu^{n+\frac{1}{2}}\right\|^2+\frac{5}{12}M_v\tau\|\nabla\ddot{e}_\xi^{n+1}\|^2+C\tau^4\int_{t^n}^{t^{n+1}}(\|u_{ttt}\|_{-1}^2+\|v_{tt}\|_{-1}^2+\|v_{ttt}\|_{-1}^2)ds\\
&\quad+C\tau((e_r^{n+1})^2+(e_r^n)^2+\|\tilde{\ddot{e}}_u^n\|^2+\|\nabla\tilde{\ddot{e}}_u^n\|^2+\|\tilde{\ddot{e}}_v^n\|^2+\|\nabla\tilde{\ddot{e}}_v^n\|^2+\|\ddot{e}_v^{n+1}-\bar{\ddot{e}}_v^{n+1}\|_{-1}^2+\|\ddot{e}_v^n-\bar{\ddot{e}}_v^n\|_{-1}^2)\\
&\quad+C\tau^4\int_{t^{n-1}}^{t^{n+1}}(\|u_{tt}\|_{H^1}^2+\|v_{tt}\|_{H^1}^2+\|u_{tt}\|_{H^3}^2+\|v_{tt}\|_{H^3}^2+|r_{tt}|^2+|r_{ttt}|^2+\|u_{ttt}\|^2+\|v_{ttt}\|^2)ds\\
&\quad+C\tau(\|\tilde{u}(t^n)\|_{m+1}^2+\|\tilde{v}(t^n)\|_{m+1}^2)h^{2m}.
\end{aligned} \tag{4.39}$$

Summing up the above inequality (4.39) from $n=1$ to k $(k\geq 1)$, ignoring some non-negative terms, we have:

$$\frac{\epsilon_u^2}{2}\left\|\nabla\ddot{e}_u^{k+1}\right\|^2+\frac{S}{2}\left\|\ddot{e}_u^{k+1}\right\|^2+\frac{\epsilon_v^2}{2}\left\|\nabla\ddot{e}_v^{k+1}\right\|^2+\frac{S}{2}\left\|\ddot{e}_v^{k+1}\right\|^2+(e_r^k)^2+\left\|\ddot{e}_v^{k+1}-\bar{\ddot{e}}_v^{k+1}\right\|_{-1}^2$$

$$+\frac{1}{2}M_u\tau\sum_{n=1}^{k}\left\|\nabla\ddot{e}_{\mu}^{n+\frac{1}{2}}\right\|^2+\frac{1}{2}M_v\tau\sum_{n=1}^{k}\left\|\nabla\ddot{e}_{\xi}^{n+\frac{1}{2}}\right\|^2$$
$$\le\frac{\epsilon_u^2}{2}\left\|\nabla\ddot{e}_u^1\right\|^2+\frac{S}{2}\left\|\ddot{e}_u^1\right\|^2+\frac{\epsilon_v^2}{2}\left\|\nabla\ddot{e}_v^1\right\|^2+\frac{S}{2}\left\|\ddot{e}_v^1\right\|^2+(e_r^1)^2+\left\|\ddot{e}_v^1-\bar{\ddot{e}}_v^1\right\|_{-1}^2$$
$$+C\tau\sum_{n=0}^{k}((e_r^n)^2+\|\ddot{e}_u^n\|^2+\|\nabla\ddot{e}_u^n\|^2+\|\ddot{e}_v^n\|^2+\|\nabla\ddot{e}_v^n\|^2+\left\|\ddot{e}_v^n-\bar{\ddot{e}}_v^n\right\|_{-1}^2)ds$$
$$+C\tau^4\int_0^{t^k}(\|u_{tt}\|_{H^1}^2+\|v_{tt}\|_{H^1}^2+\|u_{tt}\|_{H^3}^2+\|v_{tt}\|_{H^3}^2+\|u_{ttt}\|^2+\|v_{ttt}\|^2+|r_{tt}|^2+|r_{ttt}|^2)$$
$$+C\tau^4\int_0^{t^k}(\|u_{ttt}\|_{-1}^2+\|v_{tt}\|_{-1}^2+\|v_{ttt}\|_{-1}^2)ds+Ch^{2m}. \tag{4.40}$$

Starting from (3.9)-(3.13), the error estimates of the first step can be obtained by using a similar procedure described above

$$\frac{\epsilon_u^2}{2}(\|\nabla\ddot{e}_u^1\|^2-\|\nabla\ddot{e}_u^0\|^2+\|\nabla(\ddot{e}_u^1-\ddot{e}_u^0)\|^2)+\frac{S}{2}(\|\ddot{e}_u^1\|^2-\|\ddot{e}_u^0\|^2+\|\ddot{e}_u^1-\ddot{e}_u^0\|^2)+M_u\tau\left\|\nabla\ddot{e}_{\mu}^{\frac{1}{2}}\right\|^2$$
$$+\frac{\epsilon_v^2}{2}(\|\nabla\ddot{e}_v^1\|^2-\|\nabla\ddot{e}_v^0\|^2+\|\nabla(\ddot{e}_v^1-\ddot{e}_v^0)\|^2)+\frac{S}{2}(\|\ddot{e}_v^1\|^2-\|\ddot{e}_v^0\|^2+\|\ddot{e}_v^1-\ddot{e}_v^0\|^2)+M_v\tau\left\|\nabla\ddot{e}_{\xi}^{\frac{1}{2}}\right\|^2$$
$$+(e_r^1)^2-(e_r^0)^2+\left\|\ddot{e}_v^1-\bar{\ddot{e}}_v^1\right\|_{-1}^2-\left\|\ddot{e}_v^0-\bar{\ddot{e}}_v^0\right\|_{-1}^2$$
$$\le\frac{1}{4}M_u\tau\left\|\nabla\ddot{e}_{\mu}^{\frac{1}{2}}\right\|^2+\frac{1}{2}M_v\tau\left\|\nabla\ddot{e}_{\xi}^{\frac{1}{2}}\right\|^2+C\tau((e_r^1)^2+\|\ddot{e}_u^0\|_{H^1}^2+\|\ddot{e}_v^0\|_{H^1}^2+\left\|\ddot{e}_v^1-\bar{\ddot{e}}_v^1\right\|_{-1}^2)+Ch^{2m}$$
$$+C\tau^4\int_{t^0}^{t^1}(\|u_{ttt}\|^2+\|v_{ttt}\|^2+\|u_{tt}\|_{H^1}^2+\|v_{tt}\|_{H^1}^2+\|u_{ttt}\|_{-1}^2+\|v_{ttt}\|_{-1}^2+|r_{ttt}(s)|^2)ds. \tag{4.41}$$

Note that $u_N^0=\prod_N u(t^0)$, $v_N^0=\prod_N v(t^0)$, we have $\ddot{e}_u^0=\ddot{e}_v^0=0$. Substituting (4.41) into (4.40), and applying Gronwall's inequality, there exists a positive constant τ_1 such that

$$\frac{\epsilon_u^2}{2}\left\|\nabla\ddot{e}_u^{k+1}\right\|^2+\frac{S}{2}\left\|\ddot{e}_u^{k+1}\right\|^2+\frac{\epsilon_v^2}{2}\left\|\nabla\ddot{e}_v^{k+1}\right\|^2+\frac{S}{2}\left\|\ddot{e}_v^{k+1}\right\|^2+\left\|\ddot{e}_v^{k+1}-\bar{\ddot{e}}_v^{k+1}\right\|_{-1}^2+(e_r^{k+1})^2$$
$$+\frac{1}{2}M_u\tau\sum_{n=0}^{k}\left\|\nabla\ddot{e}_{\mu}^{n+\frac{1}{2}}\right\|^2+\frac{1}{2}M_v\tau\sum_{n=0}^{k}\left\|\nabla\ddot{e}_{\xi}^{n+\frac{1}{2}}\right\|^2\lesssim\tau^4+h^{2m}, \tag{4.42}$$

where $\tau<\tau_1$ and $k=0,1,2,\cdots,[T_{max}/\tau]-1$.

Step 4. To prove the L^∞ boundedness of v_N^{k+1}, we need to obtain the H^2 boundedness of e_v^{k+1} first. Combining the H^2 regularity conclusion for the elliptic equation, (4.19), Poincaré inequality, projection error (3.3) and (4.42), we obtain

$$\begin{aligned}\left\|e_v^{k+1}\right\|_{H^2}&\lesssim\left\|e_v^{k+1}\right\|+\left\|\Delta e_v^{k+1}\right\|\\&\lesssim\left\|e_v^{k+1}\right\|\\&\quad+\left\|-\ddot{e}_{\xi}^{k+\frac{1}{2}}-\frac{\epsilon_v^2}{2}\Delta e_v^k+S\hat{\ddot{e}}_v^{k+\frac{1}{2}}+r_N^{k+\frac{1}{2}}G(\tilde{u}_N^k,\tilde{v}_N^k)-\hat{r}(t^{k+\frac{1}{2}})G(\tilde{u}(t^k),\tilde{v}(t^k))+R_{\xi}^{k+\frac{1}{2}}\right\|\\&\lesssim\left\|e_v^{k+1}\right\|+\left\|\ddot{e}_{\xi}^{k+\frac{1}{2}}\right\|+\left\|\Delta e_v^k\right\|+\left\|\hat{\ddot{e}}_v^{k+\frac{1}{2}}\right\|\\&\quad+\left\|r_N^{k+\frac{1}{2}}G(\tilde{u}_N^k,\tilde{v}_N^k)-\hat{r}(t^{k+\frac{1}{2}})G(\tilde{u}(t^k),\tilde{v}(t^k))\right\|+\left\|R_{\xi}^{k+\frac{1}{2}}\right\|\\&\lesssim\left\|\ddot{e}_v^{k+1}\right\|+\left\|\check{e}_v^{k+1}\right\|+\left\|\nabla\ddot{e}_{\xi}^{k+\frac{1}{2}}\right\|+\left\|\Delta e_v^k\right\|+\left\|\hat{\ddot{e}}_v^{k+\frac{1}{2}}\right\|+\left\|R_{\xi}^{k+\frac{1}{2}}\right\|\\&\quad+\left\|G(\tilde{u}_N^k,\tilde{v}_N^k)-G(\tilde{u}(t^k),\tilde{v}(t^k))\right\|+|\hat{e}_r^{k+\frac{1}{2}}|\end{aligned}$$

$$\lesssim \tau^{\frac{3}{2}} + h^m,$$

where $\|\Delta e_v^k\| \lesssim \tau^{\frac{3}{2}} + h^m$ is guaranteed by the projection error (3.3) and

$$\begin{aligned}\|\Delta \ddot{e}_v^1\| &\lesssim \|-\ddot{e}_\xi^1 + S\ddot{e}_v^1 + r_N^1 G(u_N^0, v_N^0) - r(t^1)G(u(t^0), v(t^0)) + R_\xi^1\| \\ &\lesssim \|\nabla \ddot{e}_\xi^1\| + \|\ddot{e}_v^1\| + \|r_N^1 G(u_N^0, v_N^0) - r(t^1)G(u(t^0), v(t^0))\| + \|R_\xi^1\| \\ &\lesssim \tau^{\frac{3}{2}} + h^m.\end{aligned}$$

The L^2 boundedness of $R_\xi^{k+\frac{1}{2}}$ and $G(\tilde{u}_N^k, \tilde{v}_N^k) - G(\tilde{u}(t^k), \tilde{v}(t^k))$ can be obtained similar to (4.34) and (B.1) in Appendix B. In fact, we have

$$\left\|R_\xi^{k+\frac{1}{2}}\right\|^2 \lesssim \tau^3 \int_{t^{k-1}}^{t^{k+1}} \left(\|u_{tt}\|^2 + \|\Delta v_{tt}\|^2 + \|v_{tt}\|^2 + |r_{tt}|^2\right) ds,$$

$$\|G(\tilde{u}_N^k, \tilde{v}_N^k) - G(\tilde{u}(t^k), \tilde{v}(t^k))\| \lesssim \|\tilde{e}_u^k\| + \|\tilde{e}_v^k\| \lesssim \tau^{\frac{3}{2}} + h^m.$$

Then, we can obtain

$$\begin{aligned}\|v_N^{k+1}\|_{L^\infty} &\le \|e_v^{k+1}\|_{L^\infty} + \|v(t^{k+1})\|_{L^\infty} \lesssim \|e_v^{k+1}\|_{H^1} + \|v(t^{k+1})\|_{L^\infty} \\ &\le C_2\tau^2 + C_2 h^m + \|v(t^{k+1})\|_{L^\infty} \le C, \quad for\ d=2,\end{aligned}$$

$$\begin{aligned}\|v_N^{k+1}\|_{L^\infty} &\le \|e_v^{k+1}\|_{L^\infty} + \|v(t^{k+1})\|_{L^\infty} \lesssim \|e_v^{k+1}\|_{H^2} + \|v(t^{k+1})\|_{L^\infty} \\ &\le C_3\tau^{\frac{3}{2}} + C_3 h^m + \|v(t^{k+1})\|_{L^\infty} \le C, \quad for\ d=3,\end{aligned}$$

where $\tau \le \tau_2 = min\{\sqrt{1/C_2}, \sqrt[3]{1/C_2^2}\}$, $h \le h_2 = min\{\sqrt[m]{1/C_2}, \sqrt[m]{1/C_3}\}$. Thus, we conclude that $\tau < \tau_0 = min\{\tau_1, \tau_2\}$ and $h < h_0 = min\{h_1, h_2\}$. ∎

THEOREM 4.1. *Supposing that the exact solutions of system (3.2) satisfy the regularity assumption (4.6), then, we have*

$$\frac{\epsilon_u^2}{2}\|\nabla e_u^k\|^2 + \frac{S}{2}\|e_u^k\|^2 + \frac{\epsilon_v^2}{2}\|\nabla e_v^k\|^2 + \frac{S}{2}\|e_v^k\|^2 + \|e_v^k - \bar{e}_v^k\|_{-1}^2 + (e_r^k)^2 \lesssim \tau^4 + h^{2m}, \quad (4.43)$$

where $k = 0, 1, 2, \cdots, [T_{max}/\tau]$.

Proof. Denote

$$I_k = \frac{\epsilon_u^2}{2}\|\nabla e_u^k\|^2 + \frac{S}{2}\|e_u^k\|^2 + \frac{\epsilon_v^2}{2}\|\nabla e_v^k\|^2 + \frac{S}{2}\|e_v^k\|^2 + \|e_v^k - \bar{e}_v^k\|_{-1}^2 + (e_r^k)^2.$$

Lemma 4.3 indicates that $I_n \lesssim \tau^4 + h^{2m}$ for $\tau < \tau_0$ and $h < h_0$. For other cases, considering the energy stability Theorem 3.1, we have

$$I_n \le C \le \frac{C}{h_0^{2m}} h^{2m} \lesssim \tau^4 + h^{2m}, for\ \tau < \tau_0, h \ge h_0,$$

$$I_n \le C \le \frac{C}{\tau_0^4} \tau^4 \lesssim \tau^4 + h^{2m}, for\ \tau \ge \tau_0, h < h_0,$$

$$I_n \le C \le \frac{C}{2\tau_0^4} \tau^4 + \frac{C}{2h_0^{2m}} h^{2m} \lesssim \tau^4 + h^{2m}, for\ \tau \ge \tau_0, h \ge h_0.$$

Thus, the proof is completed. ∎

τ	$\|e_u\|$	rate	$\|e_u\|_\infty$	rate
τ_0	$3.0168E-4$	/	$3.8673E-5$	/
$\tau_0/2$	$7.7624E-5$	1.96	$1.0044E-5$	1.94
$\tau_0/2^2$	$1.9708E-5$	1.98	$2.5625E-6$	1.97
$\tau_0/2^3$	$4.9636E-6$	1.99	$6.4704E-7$	1.99
$\tau_0/2^4$	$1.2424E-6$	2.00	$1.6217E-7$	2.00
$\tau_0/2^5$	$3.0760E-7$	2.01	$4.0176E-8$	2.01

TABLE 5.1. *Time errors and convergence rates of u at $T_{max}=0.025$ for the SAV/CN scheme with the time step $\tau=1\times10^{-3}/2^k$, $k=0,1,2,3,4,5$.*

τ	$\|e_v\|$	rate	$\|e_v\|_\infty$	rate
τ_0	$4.1951E-5$	/	$4.6534E-6$	/
$\tau_0/2$	$1.0500E-5$	2.00	$1.1639E-6$	2.00
$\tau_0/2^2$	$2.6260E-6$	2.00	$2.9100E-7$	2.00
$\tau_0/2^3$	$6.5622E-7$	2.00	$7.2705E-8$	2.00
$\tau_0/2^4$	$1.6360E-7$	2.00	$1.8124E-8$	2.00
$\tau_0/2^5$	$4.0421E-8$	2.02	$4.4778E-9$	2.02

TABLE 5.2. *Time errors and convergence rates of v at $T_{max}=0.025$ for the SAV/CN scheme with the time step $\tau=1\times10^{-3}/2^k$, $k=0,1,2,3,4,5$.*

5. Numerical experiments

In this section, we give several numerical examples to demonstrate the effectiveness of the SAV/CN scheme. First, we present convergence tests in time and space through mesh refinement experiments. Then, we validate the energy dissipation and mass conservation of the system. Finally we show some phase transition experiments.

5.1. Accuracy test. Here, we consider the two-dimensional problem with $\Omega=[0,L]^2$. In our simulations, we choose the initial values $u^0=0.25cos(x)sin(y)$, $v^0=0.25sin(x)cos(y)+0.1$. The parameters are fixed as follows: $L=4\pi$, $M_u=1$, $M_v=0.05$, $\alpha=0.01$, $\beta=-0.9$, $\sigma=100$, $\epsilon_u=0.05$, $\epsilon_v=0.05$, $S=20$ and $C_0=5000$.

For time accuracy, we fix the space step size h as $2^{-7}L$. We compute the numerical solutions with time steps $\tau=\tau_0/2^k$ ($\tau_0=1\times10^{-3}$), $k=0,1,2,3,4,5$ at $T_{max}=0.025$, and regard the numerical solution calculated with a very small time step $\tau=\tau_0/2^8$ as the "exact" solution. The second-order accuracy of the SAV/CN scheme in the time direction is shown in Tables 5.1-5.2. For space accuracy, we choose the time step $\tau=2\times10^{-5}$. Then, we compute the numerical solutions with grid numbers $N=8\times2^k$, $k=0,1,2,3,4$ at $T_{max}=0.1$, and regard the numerical solution calculated with the grid number $N=2^{10}$ as the "exact" solution. Tables 5.3-5.4 present the L^2 (or L^∞) errors of u and v, which indicates that the spatial error converges exponentially.

5.2. Energy dissipation and mass conservation. Although the SAV/CN scheme is unconditionally energy stable, we want to select an appropriate time step to guarantee accuracy with a smaller computational effort. We set the space step size as $h=2^{-7}$ and select different τ as 1×10^{-4}, 5×10^{-5}, 2×10^{-5}, 1×10^{-5} and 5×10^{-6}. The time evolution curves of the modified energy under different τ are shown in Figure 5.1(a). It can be observed that the modified energies all decrease with time. The curves under time step size $\tau=2\times10^{-5}$, 1×10^{-5} and 5×10^{-6} coincide. Thus, we choose $\tau\le2\times10^{-5}$

N	$\|e_u\|$	rate	$\|e_u\|_\infty$	rate
8	$7.9300E-2$	/	$1.3420E-2$	/
16	$9.1807E-3$	3.11	$1.9858E-3$	2.76
32	$7.6628E-4$	3.58	$1.9197E-4$	3.37
64	$1.3122E-6$	9.19	$5.0081E-7$	8.58
128	$2.8708E-10$	12.16	$1.5039E-10$	11.70

TABLE 5.3. *Spatial errors and convergence rates of u at $T_{max}=0.1$ for the SAV/CN scheme with the grid numbers $N=8\times 2^k$, $k=0,1,2,3,4$.*

N	$\|e_v\|$	rate	$\|e_v\|_\infty$	rate
8	$3.9686E-4$	/	$5.1184E-5$	/
16	$7.7772E-5$	2.35	$1.3927E-5$	1.88
32	$9.7908E-6$	2.99	$2.3650E-6$	2.56
64	$5.0039E-8$	7.61	$1.4204E-8$	7.38
128	$1.0802E-11$	12.18	$6.9536E-12$	11.00

TABLE 5.4. *Spatial errors and convergence rates of v at $T_{max}=0.1$ for the SAV/CN scheme with the grid numbers $N=8\times 2^k$, $k=0,1,2,3,4$.*

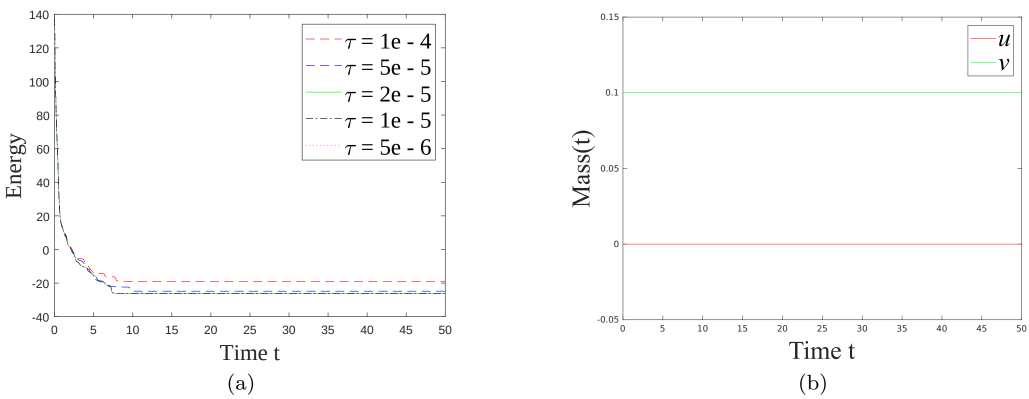

FIG. 5.1. *(a) Evolution of the modified energy with different τ; (b) Mass evolution of u and v.*

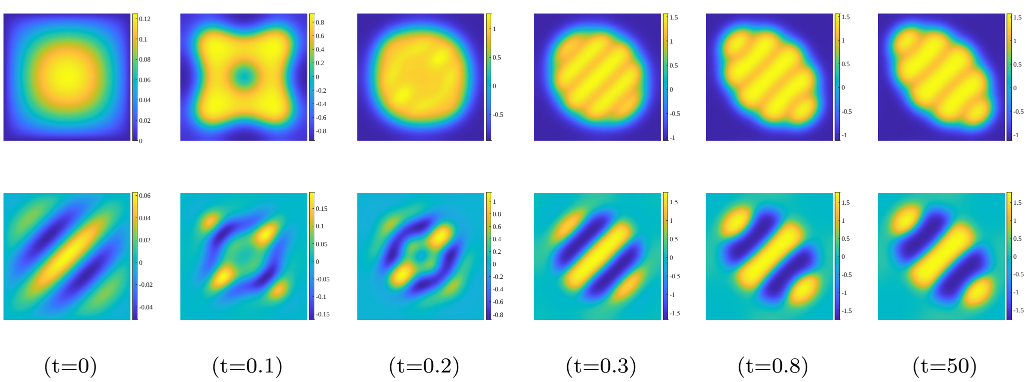

FIG. 5.2. *Evolution of u (top) and v (bottom) with parameters $\epsilon_u=\epsilon_v=0.05, M_u=1, M_v=0.05, \alpha=0.01, \beta=-0.9, \sigma=100, S=10, \tau=2\times 10^{-5}$ and $h=2^{-7}$.*

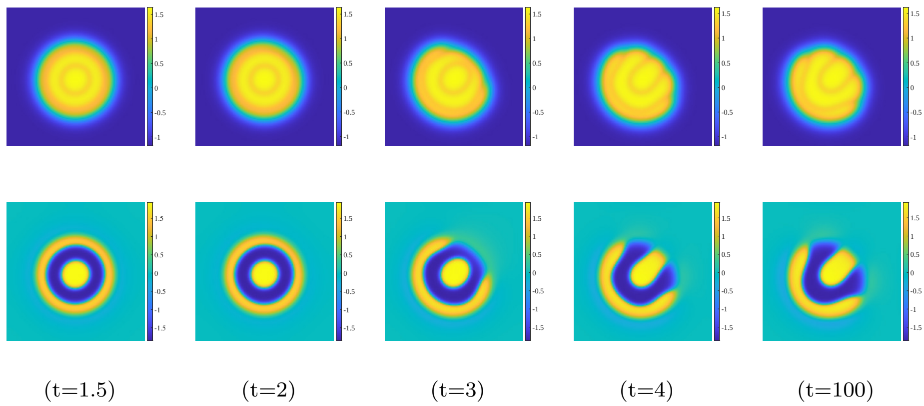

FIG. 5.3. *Evolution of u (top) and v (bottom) with parameters* $\epsilon_u = 0.05, \epsilon_v = 0.02$, $M_u = 1$, $M_v = 0.05$, $\alpha = 0.01$, $\beta = -0.9$, $\sigma = 160$, $S = 10$, $\tau = 2 \times 10^{-5}$ *and* $h = 2^{-7}$.

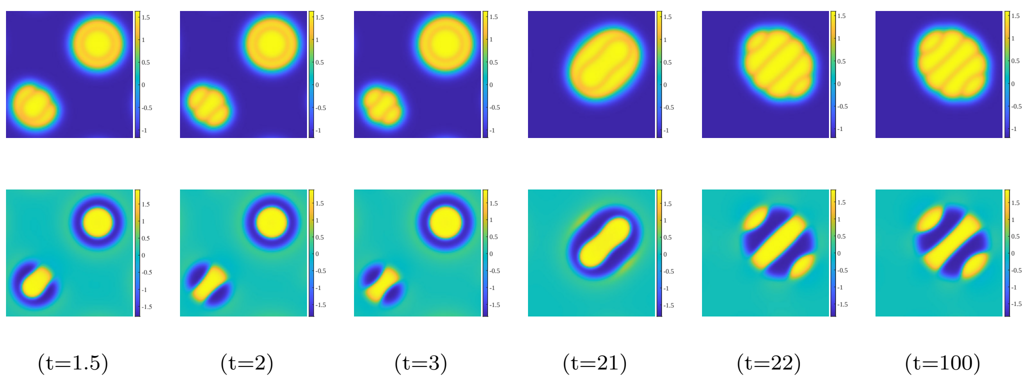

FIG. 5.4. *Evolution of u (top) and v (bottom) with parameters* $\epsilon_u = 0.04, \epsilon_v = 0.02$, $M_u = 1$, $M_v = 0.05$, $\alpha = 0.01$, $\beta = -0.9$, $\sigma = 160$, $S = 10$, $\tau = 2 \times 10^{-5}$ *and* $h = 2^{-7}$.

for the later simulations. For the case of $\tau = 2 \times 10^{-5}$, we present the corresponding mass evolution of u and v in Figure 5.1(b). The lines are located on the horizontal line, which indicates that the fully discrete scheme maintains the property of mass conservation.

5.3. Phase transition. We simulate the transformation process of typical particles, such as stacked lamellae and onion-like structures. First, we choose the initial values $u^0 = sin(2x(x-1)y(y-1))$ and $v^0 = cos(10(x-y))x(x-1)y(y-1)$. The parameters are selected as follows. $\epsilon_u = \epsilon_v = 0.05$, $M_u = 1$, $M_v = 0.05$, $\alpha = 0.01$, $\beta = -0.9$, $\sigma = 100$, $S = 10$. The time and space steps are fixed as $\tau = 2 \times 10^{-5}$ and $h = 2^{-7}$ in simulations in this subsection. The evolution of u (top) and v (bottom) are presented in Figure 5.2.

As shown in Figure 5.2, the macrophase separation between homopolymers and copolymer forms in the initial state, promoting the aggregation of block copolymers. With time evolution, microphase separation occurs due to the different chemical properties of the A- and B-blocks. Finally, stacked lamellae form at $t = 0.8$.

Then, we apply the random initial values $u^0 = -0.5 + 0.01rand(x,y)$, $v^0 = 0.01rand(x,y)$, for numerical simulation with parameters $L = 1$, $h = 2^{-7}$, $\tau = 0.002$, $M_u = 1$, $M_v = 0.05$, $\alpha = 0.01$, $\beta = -0.9$, $\sigma = 160$, $\epsilon_v = 0.02$, $S = 10$, $C_0 = 20$. The evolution of u and v under parameters $\epsilon_u = 0.05$ and $\epsilon_u = 0.04$ are presented in Figures 5.3

and 5.4, respectively.

6. Summary

In this paper, we have derived the error estimates for the SAV/CN approach of the coupled Cahn-Hilliard system in both time and space. The emphasis here is on the mathematical treatment of the nonlocal term. To the best of our knowledge, this is the first study to perform an error analysis on the Cahn-Hilliard system, in which two phase variables are coupled and the nonlocal term exists. We have also conducted some numerical experiments to demonstrate the properties of the scheme, such as the time accuracy, spatial accuracy, and mass conservation.

Acknowledgments. G. Ji is partially supported by the National Natural Science Foundation of China (Grant Nos. 11571045, 11671052 and 11871105), the State Scholarship Fund of CSC (Grant No. 201406045016).

Appendix A. The proof of Lemma 4.1.

Proof. For simplicity, we denote u, v, $E_1(u,v)+C_0$ as ϕ_i, $i=1,2$ and E_1 here. Using chain rule, we have

$$r_{tt}=-\frac{1}{4\sqrt{E_1^3}}\left(\sum_{i=1}^{2}\int_\Omega\frac{\partial E_1}{\partial\phi_i}\frac{\partial\phi_i}{\partial t}d\mathbf{x}\right)^2+\frac{1}{2\sqrt{E_1}}\sum_{i=1}^{2}\int_\Omega\left(\frac{\partial\phi_i}{\partial t}\sum_{j=1}^{2}\frac{\partial^2E_1}{\partial\phi_j\partial\phi_i}\frac{\partial\phi_j}{\partial t}+\frac{\partial E_1}{\partial\phi_i}\frac{\partial^2\phi_i}{\partial t^2}\right)d\mathbf{x},$$

$$\begin{aligned}r_{ttt}=&\frac{3}{8\sqrt{E_1^5}}\left(\sum_{i=1}^{2}\int_\Omega\frac{\partial E_1}{\partial\phi_i}\frac{\partial\phi_i}{\partial t}d\mathbf{x}\right)^3\\&-\frac{3}{4\sqrt{E_1^3}}\left(\sum_{i=1}^{2}\int_\Omega\frac{\partial E_1}{\partial\phi_i}\frac{\partial\phi_i}{\partial t}d\mathbf{x}\right)\sum_{i=1}^{2}\int_\Omega\left(\frac{\partial\phi_i}{\partial t}\sum_{j=1}^{2}\frac{\partial^2E_1}{\partial\phi_j\partial\phi_i}\frac{\partial\phi_j}{\partial t}+\frac{\partial E_1}{\partial\phi_i}\frac{\partial^2\phi_i}{\partial t^2}\right)d\mathbf{x}\\&+\frac{1}{2\sqrt{E_1}}\sum_{i=1}^{2}\int_\Omega\left(2\frac{\partial^2\phi_i}{\partial t^2}\sum_{j=1}^{2}\frac{\partial^2E_1}{\partial\phi_j\partial\phi_i}\frac{\partial\phi_j}{\partial t}+\frac{\partial\phi_i}{\partial t}\sum_{j=1}^{2}\frac{\partial^2E_1}{\partial\phi_j\partial\phi_i}\frac{\partial^2\phi_j}{\partial t^2}\right)d\mathbf{x}\\&+\frac{1}{2\sqrt{E_1}}\sum_{i=1}^{2}\int_\Omega\left(\frac{\partial\phi_i}{\partial t}\sum_{j,l=1}^{2}\frac{\partial^3E_1}{\partial\phi_j\partial\phi_l\partial\phi_i}\frac{\partial\phi_j}{\partial t}\frac{\partial\phi_l}{\partial t}+\frac{\partial E_1}{\partial\phi_i}\frac{\partial^3\phi_j}{\partial t^3}\right)d\mathbf{x}.\end{aligned}$$

For the first term, applying Hölder inequality and Soblev embedding theorem, we have

$$\begin{aligned}|r_{tt}|^2\lesssim&\left[\left(\sum_{i=1}^{2}\int_\Omega\frac{\partial E_1}{\phi_i}\frac{\partial\phi_i}{\partial t}d\mathbf{x}\right)^4+\left(\sum_{i=1}^{2}\int_\Omega\frac{\partial\phi_i}{\partial t}\sum_{j=1}^{2}\frac{\partial^2E_1}{\partial\phi_j\partial\phi_i}\frac{\partial\phi_j}{\partial t}d\mathbf{x}\right)^2+\left(\sum_{i=1}^{2}\int_\Omega\frac{\partial E_1}{\partial\phi_i}\frac{\partial^2\phi_i}{\partial t^2}d\mathbf{x}\right)^2\right]\\\lesssim&\sum_{i=1}^{2}\left(\left\|\frac{\partial\phi_i}{\partial t}\right\|_{L^4}^4+\left\|\frac{\partial^2\phi_i}{\partial t^2}\right\|^2\right)\\\lesssim&\sum_{i=1}^{2}\left(\left\|\frac{\partial\phi_i}{\partial t}\right\|_{H^1}^4+\left\|\frac{\partial^2\phi_i}{\partial t^2}\right\|^2\right).\end{aligned}\tag{A.1}$$

The second term

$$\begin{aligned}|r_{ttt}|^2\lesssim&\left(\sum_{i=1}^{2}\int_\Omega\frac{\partial E_1}{\partial\phi_i}\frac{\partial\phi_i}{\partial t}d\mathbf{x}\right)^6&&(:=A_1)\\&+C\left(\sum_{i=1}^{2}\int_\Omega\frac{\partial E_1}{\partial\phi_i}\frac{\partial\phi_i}{\partial t}d\mathbf{x}\right)^2\left(\sum_{i=1}^{2}\int_\Omega\left(\frac{\partial\phi_i}{\partial t}\sum_{j=1}^{2}\frac{\partial^2E_1}{\partial\phi_j\partial\phi_i}\frac{\partial\phi_j}{\partial t}+\frac{\partial E_1}{\partial\phi_i}\frac{\partial^2\phi_i}{\partial t^2}\right)d\mathbf{x}\right)^2&&(:=A_2)\end{aligned}$$

$$+C\left(\sum_{i=1}^{2}\int_{\Omega}\frac{\partial^2\phi_i}{\partial t^2}\sum_{j=1}^{2}\frac{\partial^2 E_1}{\partial\phi_j\partial\phi_i}\frac{\partial\phi_j}{\partial t}d\mathbf{x}\right)^2 \qquad (:=A_3)$$

$$+C\left(\sum_{i=1}^{2}\int_{\Omega}\frac{\partial\phi_i}{\partial t}\sum_{j=1}^{2}\frac{\partial^2 E_1}{\partial\phi_j\partial\phi_i}\frac{\partial^2\phi_j}{\partial t^2}d\mathbf{x}\right)^2 \qquad (:=A_4)$$

$$+C\left(\sum_{i=1}^{2}\int_{\Omega}\frac{\partial\phi_i}{\partial t}\sum_{j,l=1}^{2}\frac{\partial^3 E_1}{\partial\phi_j\partial\phi_l\partial\phi_i}\frac{\partial\phi_j}{\partial t}\frac{\partial\phi_l}{\partial t}d\mathbf{x}\right)^2 \qquad (:=A_5)$$

$$+C\left(\sum_{i=1}^{2}\int_{\Omega}\frac{\partial E_1}{\partial\phi_i}\frac{\partial^3\phi_i}{\partial t^3}d\mathbf{x}\right)^2, \qquad (:=A_6)$$

can be estimated in a similar way as (A.1) as follows

$$A_1\lesssim\sum_{i=1}^{2}\left\|\frac{\partial\phi_i}{\partial t}\right\|_{L^6}^6\lesssim\sum_{i=1}^{2}\left\|\frac{\partial\phi_i}{\partial t}\right\|_{H^1}^6, \tag{A.2}$$

$$\begin{aligned}A_2&\lesssim\left(\sum_{i=1}^{2}\int_{\Omega}|\frac{\partial\phi_i}{\partial t}|^2d\mathbf{x}\right)\left(\sum_{i,j=1}^{2}\int_{\Omega}|\frac{\partial\phi_i}{\partial t}|^2|\frac{\partial\phi_j}{\partial t}|^2d\mathbf{x}+\sum_{i=1}^{2}\int_{\Omega}|\frac{\partial^2\phi_i}{\partial t^2}|^2d\mathbf{x}\right)\\&\lesssim\left(\sum_{i=1}^{2}\left\|\frac{\partial\phi_i}{\partial t}\right\|_{L^6}^2\right)\left(\sum_{i=1}^{2}\left\|\frac{\partial\phi_i}{\partial t}\right\|_{L^6}^4+\sum_{i=1}^{2}\left\|\frac{\partial^2\phi_i}{\partial t^2}\right\|^2\right)\\&\lesssim\sum_{i=1}^{2}\left(\left\|\frac{\partial\phi_i}{\partial t}\right\|_{L^6}^8+\left\|\frac{\partial\phi_i}{\partial t}\right\|_{L^6}^4+\left\|\frac{\partial^2\phi_i}{\partial t^2}\right\|^4\right)\\&\lesssim\sum_{i=1}^{2}\left(\left\|\frac{\partial\phi_i}{\partial t}\right\|_{H^1}^8+\left\|\frac{\partial\phi_i}{\partial t}\right\|_{H^1}^4+\left\|\frac{\partial^2\phi_i}{\partial t^2}\right\|^4\right).\end{aligned} \tag{A.3}$$

A_3 and A_4 can be estimated by

$$A_3\lesssim\sum_{i,j=1}^{2}\left\|\frac{\partial^2\phi_i}{\partial t^2}\right\|^2\left\|\frac{\partial\phi_i}{\partial t}\right\|^2\lesssim\sum_{i=1}^{2}\left\|\frac{\partial^2\phi_i}{\partial t^2}\right\|^2\left\|\frac{\partial\phi_i}{\partial t}\right\|_{L^6}^2\lesssim\sum_{i=1}^{2}\left(\left\|\frac{\partial^2\phi_i}{\partial t^2}\right\|^4+\left\|\frac{\partial\phi_i}{\partial t}\right\|_{H^1}^2\right), \tag{A.4}$$

$$A_4\lesssim\sum_{i=1}^{2}\left(\left\|\frac{\partial^2\phi_i}{\partial t^2}\right\|^4+\left\|\frac{\partial\phi_i}{\partial t}\right\|_{H^1}^2\right), \tag{A.5}$$

$$\begin{aligned}A_5&\lesssim\sum_{i,j,l=1}^{2}\int_{\Omega}|\frac{\partial\phi_i}{\partial t}|^2|\frac{\partial\phi_j}{\partial t}|^2|\frac{\partial\phi_l}{\partial t}|^2d\mathbf{x}\lesssim\sum_{i,j,l=1}^{2}\int_{\Omega}(|\frac{\partial\phi_i}{\partial t}|^6+|\frac{\partial\phi_j}{\partial t}|^6+|\frac{\partial\phi_l}{\partial t}|^6)d\mathbf{x}\\&\lesssim\sum_{i=1}^{2}\left\|\frac{\partial\phi_i}{\partial t}\right\|_{H^1}^6,\end{aligned} \tag{A.6}$$

$$A_6\lesssim\sum_{i=1}^{2}\left\|\nabla\frac{\partial E_1}{\partial\phi_i}\right\|_{L^\infty}^2\int_{\Omega}|(-\Delta)^{-1/2}\frac{\partial^3\phi_i}{\partial t^3}|^2d\mathbf{x}\lesssim\sum_{j=1}^{2}\|\nabla\phi_j\|_{L^\infty}^2\sum_{i=1}^{2}\left\|\frac{\partial^3\phi_i}{\partial t^3}\right\|_{-1}^2. \tag{A.7}$$

Combining Equation (A.1)-(A.7), the proof of Lemma 4.1 is completed. ∎

Appendix B. The proof of Lemma 4.2.

Proof. Note that

$$R_u^{n+\frac{1}{2}}=u_t(t^{n+\frac{1}{2}})\tau-(u(t^{n+1})-u(t^n))$$

$$=\frac{1}{2}\int_{t^{n+1}}^{t^{n+\frac{1}{2}}}(t^{n+1}-s)^2u_{ttt}(s)ds+\frac{1}{2}\int_{t^n}^{t^{n+\frac{1}{2}}}(t^n-s)^2u_{ttt}(s)ds,$$

we have

$$\begin{aligned}\left\|R_u^{n+\frac{1}{2}}\right\|_{-1}^2&\le\frac{1}{2}\left\|\int_{t^{n+1}}^{t^{n+\frac{1}{2}}}(t^{n+1}-s)^2u_{ttt}(s)ds+\int_{t^n}^{t^{n+\frac{1}{2}}}(t^n-s)^2u_{ttt}(s)ds\right\|_{-1}^2\\&\le\int_\Omega\left(\int_{t^{n+1}}^{t^{n+\frac{1}{2}}}(t^n-s)^4ds+\int_{t^n}^{t^{n+\frac{1}{2}}}(t^n-s)^4ds\right)\left(\int_{t^n}^{t^{n+1}}((-\Delta)^{-\frac{1}{2}}u_{ttt}(s))^2ds\right)d\mathbf{x}\\&\lesssim\tau^5\int_{t^n}^{t^{n+1}}\|u_{ttt}(s)\|_{-1}^2ds.\end{aligned}$$

Similarly, we have

$$\begin{aligned}\left\|R_v^{n+\frac{1}{2}}\right\|_{-1}^2&\lesssim\left\|v_t(t^{n+\frac{1}{2}})\tau-(v(t^{n+1})-v(t^n))\right\|_{-1}^2+\tau^2\left\|v(t^{n+\frac{1}{2}})-\hat{v}(t^{n+\frac{1}{2}})\right\|_{-1}^2\\&\lesssim\tau^5\int_{t^n}^{t^{n+1}}(\|v_{ttt}\|_{-1}^2+\|v_{tt}\|_{-1}^2)ds,\end{aligned}$$

$$\begin{aligned}\left\|\nabla R_\mu^{n+\frac{1}{2}}\right\|^2&\lesssim\left\|\nabla^3(u(t^{n+\frac{1}{2}})-\hat{u}(t^{n+\frac{1}{2}}))\right\|^2+\left\|\nabla(u(t^{n+\frac{1}{2}})-\hat{u}(t^{n+\frac{1}{2}}))\right\|^2\\&\quad+\left\|\nabla H(\tilde{u}(t^n),\tilde{v}(t^n))-\nabla H(u(t^{n+\frac{1}{2}}),v(t^{n+\frac{1}{2}}))\right\|^2+|\hat{r}(t^{n+\frac{1}{2}})-r(t^{n+\frac{1}{2}})|^2\\&\lesssim\tau^3\int_{t^{n-1}}^{t^{n+1}}(\left\|\nabla^3u_{tt}\right\|^2+\|\nabla u_{tt}\|^2+\|u_{tt}\|_{H^1}^2+\|v_{tt}\|_{H^1}^2)ds+\tau^3\int_{t^n}^{t^{n+1}}|r_{tt}|^2ds\\&\lesssim\tau^3\int_{t^{n-1}}^{t^{n+1}}(\|u_{tt}\|_{H^1}^2+\|v_{tt}\|_{H^1}^2+\|u_{tt}\|_{H^3}^2+|r_{tt}|^2)ds,\end{aligned}$$

$$\begin{aligned}\left\|\nabla R_\xi^{n+\frac{1}{2}}\right\|^2&\lesssim\tau^3\int_{t^n}^{t^{n+1}}\|v_{tt}\|_{H^1}^2+\|v_{tt}\|_{H^3}^2+|r_{tt}|^2ds+\tau^3\int_{t^{n-1}}^{t^{n+1}}\|u_{tt}\|_{H^1}^2+\|v_{tt}\|_{H^1}^2ds\\&\lesssim\tau^3\int_{t^{n-1}}^{t^{n+1}}(\|u_{tt}\|_{H^1}^2+\|v_{tt}\|_{H^1}^2+\|v_{tt}\|_{H^3}^2+|r_{tt}|^2)ds,\end{aligned}\tag{B.1}$$

$$\begin{aligned}|R_r^{n+\frac{1}{2}}|^2&\lesssim\left\|u(t^{n+1})-u(t^n)-u_t(t^{n+\frac{1}{2}})\tau\right\|^2+\left\|v(t^{n+1})-v(t^n)-v_t(t^{n+\frac{1}{2}})\tau\right\|^2\\&\quad+\tau^2\|u_t\|_{L^\infty(0,T,H^{-1})}^2\left\|\nabla H(u(t^{n+\frac{1}{2}}),v(t^{n+\frac{1}{2}}))-\nabla H(\tilde{u}(t^n),\tilde{v}(t^n))\right\|^2\\&\quad+\tau^2\|v_t\|_{L^\infty(0,T,H^{-1})}^2\left\|\nabla G(u(t^{n+\frac{1}{2}}),v(t^{n+\frac{1}{2}}))-\nabla G(\tilde{u}(t^n),\tilde{v}(t^n))\right\|^2\\&\quad+\tau^5\int_{t^n}^{t^{n+1}}|r_{ttt}(s)|^2ds\\&\lesssim\tau^5\int_{t^{n-1}}^{t^{n+1}}(\|u_{ttt}\|^2+\|v_{ttt}\|^2+\|u_{tt}\|_{H^1}^2+\|v_{tt}\|_{H^1}^2+|r_{ttt}(s)|^2)ds.\end{aligned}$$

∎

REFERENCES

[1] P. Lambooy, T.P. Russell, G.J. Kellogg, A.M. Mayes, P.D. Gallagher, and S.K. Satija, *Observed frustration in confined block copolymers*, Phys. Rev. Lett., 72:2899–2902, 1994. 1
[2] Q. Wang, S.K. Nath, M.D. Graham, P.F. Nealey, and J.J. De Pablo, *Symmetric diblock copolymer thin films confined between homogeneous and patterned surfaces: simulations and theory*, J. Chem. Phys., 112:9996–10010, 2000. 1
[3] Q. Wang, P.F. Nealey, and J.J. De Pablo, *Monte carlo simulations of asymmetric diblock copolymer thin films confined between two homogeneous surfaces*, Macromolecules, 34:3458–3470, 2001. 1
[4] H. Xiang, K. Shin, T. Kim, S.I. Moon, T.J. Mccarthy, and T.P. Russell, *Block copolymers under cylindrical confinement*, Macromolecules, 37:5660–5664, 2004. 1
[5] H. Xiang, K. Shin, T. Kim, S.I. Moon, T.J. Mccarthy, and T.P. Russell, *The influence of confinement and curvature on the morphology of block copolymers*, J. Polym. Sci. Part B Polym. Phys., 43:3377–3383, 2005. 1
[6] Y. Wu, G. Cheng, K. Katsov, S.W. Sides, J. Wang, J. Tang, G.H. Fredrickson, M. Moskovits, and G.D. Stucky, *Composite mesostructures by nano-confinement*, Nature Mater., 3:816–822, 2004. 1
[7] W. Li, R.A. Wickham, and R.A. Garbary, *Phase diagram for a diblock copolymer melt under cylindrical confinement*, Macromolecules, 39:806–811, 2006. 1
[8] A.C. Arsenault, D.A. Rider, N. Tétreault, J.I.-L. Chen, N. Coombs, G.A. Ozin, and I. Manners, *Block copolymers under periodic, strong three-dimensional confinement*, J. Am. Chem. Soc., 127:9954–9955. 2005. 1
[9] T. Higuchi, A. Tajima, K. Motoyoshi, H. Yabu, and M. Shimomura, *Frustrated phases of block copolymers in nanoparticles*, Angew. Chem., Int. Ed., 47:8044–8046, 2008. 1
[10] Y. Kim, A. Kumagai, X. Hu, A.-C. Shi, B. Li, H. Jinnai, and K. Char, *Self-assembled morphologies of lamella-forming block copolymers confined in conical nanopores*, Macromolecules, 52:4803–4811, 2019. 1
[11] B. Yu, B. Li, Q. Jin, D. Ding, and A.-C. Shi, *Self-assembly of symmetric diblock copolymers confined in spherical nanopores*, Macromolecules, 40:9133–9142, 2007. 1
[12] P. Chen, H. Liang, and A.-C. Shi, *Microstructures of a cylinder-forming diblock copolymer under spherical confinement*, Macromolecules, 41:8938–8943, 2008. 1
[13] B. Yu, B. Li, Q. Jin, D. Ding, and A.-C. Shi, *Confined self-assembly of cylinder-forming diblock copolymers: effects of confining geometries*, Soft Matter, 7:10227–10240, 2011. 1
[14] J.Y. Cheng, C.A. Ross, H.I. Smith, and E.L. Thomas, *Templated self-assembly of block copolymers: top-down helps bottom-up*, Adv. Mater., 18:2505–2521, 2006. 1
[15] H. Yabu, *Self-organized precipitation: an emerging method for preparation of unique polymer particles*, Polym. J., 45:261–268, 2013. 1
[16] T. Higuchi, A. Tajima, H. Yabu, and M. Shimomura, *Spontaneous formation of polymer nanoparticles with inner micro-phase separation structures*, Soft Matter, 4:1302–1305, 2008. 1
[17] P. Chi, Z. Wang, B. Li, and A.-C. Shi, *Soft confinement-induced morphologies of diblock copolymers*, Langmuir, 27:11683–11689, 2011. 1
[18] N. Yan, Y.T. Zhu, and W. Jiang, *Self-assembly of AB diblock copolymer confined in a soft nanodroplet: a combination study by Monte carlo simulation and experiment*, J. Phys. Chem. B, 120:12023–12029, 2016. 1
[19] Q. Cheng, C. Liu, and J. Shen, *A new Lagrange Multiplier approach for gradient flows*, Comput. Meth. Appl. Mech. Eng., 367:113070, 2020. 1
[20] E. Avalos, T. Teramoto, H. Komiyama, H. Yabu, and Y. Nishiura, *Transformation of block copolymer nanoparticles from ellipsoids with striped lamellae into onionlike spheres and dynamical control via coupled Cahn-Hilliard equations*, ACS Omega, 3:1304–1314, 2018. 1, 2
[21] E. Avalos, T. Higuchi, T. Teramoto, H. Yabu, and Y. Nishiura, *Frustrated phases under three-dimensional confinement simulated by a set of coupled Cahn-Hilliard equations*, Soft Matter, 12:5905–5914, 2016. 1, 2
[22] Q. Li and L. Mei, *Efficient, decoupled, and second-order unconditionally energy stable numerical schemes for the coupled Cahn-Hilliard system in copolymer/homopolymer mixtures*, Comput. Phys. Commun., 260:107290, 2021. 1, 2, 3, 3
[23] S. Kirkpatrick, C.D. Gelatt, and M.P. Vecchi, *Optimization by simulated annealing*, Science, 220:671–680, 1983. 1
[24] G.S. Grest, C.M. Soukoulis, and K. Levin, *Cooling-rate dependence for the spin-glass ground-state energy: implications for optimization by simulated annealing*, Phys. Rev. Lett., 56:1148–1151, 1986. 1
[25] G.H. Fredrickson, *The Equilibrium Theory of Inhomogeneous Polymers*, Oxford University Press, 2006. 1

[26] M.W. Matsen and M. Schick, *Stable and unstable phases of a diblock copolymer melt*, Phys. Rev. Lett., 72:2660–2663, 1994. 1

[27] M.W. Matsen, *The standard Gaussian model for block copolymer melts*, J. Phys.: Condens. Matter, 14:R21–R47, 2002. 1

[28] T. Ohta and A. Ito, *Dynamics of phase separation in copolymer-homopolymer mixtures*, Phys. Rev. E, 52:5250–5260, 1995. 1

[29] R. Choksi and X. Ren, *Diblock copolymer/homopolymer blends: derivation of a density functional theory*, Phys. D, 203:100–119, 2005. 1

[30] K. Glasner, *Multilayered equilibria in a density functional model of copolymer-solvent mixtures*, SIAM J. Math. Anal., 49:1593–1620, 2017. 1

[31] D.J. Eyre, *Unconditionally gradient stable time marching the Cahn-Hilliard equation*, in J.W. Bullard, L.-Q. Chen, R.K. Kalia, and A.M. Stoneham (ed.), Computational and Mathematical Models of Microstructural Evolution, Mater. Res. Soc. Symp. Proc., 529:39–46, 1998. 1

[32] C. Wang, Z. Guan, J.S. Lowengrub, and S.M. Wise, *Second order convex splitting schemes for periodic nonlocal Cahn-Hilliard and Allen-Cahn equations*, J. Comput. Phys., 277:48–71, 2014. 1

[33] C. Wang and S.M. Wise, *An energy stable and convergent finite-difference scheme for the modified phase field crystal equation*, SIAM J. Numer. Anal., 49(3):945–969, 2011. 1

[34] A.J. Salgado, R.H. Nochetto, and I. Tomas, *A diffuse interface model for two-phase ferrofluid flows*, Comput. Methods Appl. Mech. Eng., 309:497–531, 2016. 1

[35] J. Shen, C. Liu, and X. Yang, *Dynamics of defect motion in nematic liquid crystal flow: modeling and numerical simulations*, Commun. Comput. Phys., 2:1184–1198, 2007. 1

[36] J. Shen and X. Yang, *Decoupled, energy stable schemes for phase-field models of two-phase incompressible flows*, SIAM J. Numer. Anal., 53:279–296, 2015. 1

[37] X. Yang, *Linear, first and second-order, unconditionally energy stable numerical schemes for the phase field model of homopolymer blends*, J. Comput. Phys., 327:294–316, 2016. 1

[38] Q. Cheng, X. Yang, and J. Shen, *Efficient and accurate numerical schemes for a hydro-dynamically coupled phase field diblock copolymer model*, J. Comput. Phys., 341:44–60, 2017. 1

[39] J. Xu, J. Shen, and J. Yang, *A new class of efficient and robust energy stable schemes for gradient flows*, SIAM Rev., 61:474–506, 2019. 1

[40] F. Guillén-González, and G. Tierra, *On linear schemes for a Cahn-Hilliard diffuse interface model*, J. Comput. Phys., 234:140–171, 2013. 1

[41] H. Chen, J. Mao, and J. Shen, *Optimal error estimates for the scalar auxiliary variable finite-element schemes for gradient flows*, Numer. Math., 145:167–196, 2020. 1

[42] J. Shen, J. Xu, and J. Yang, *The scalar auxiliary variable (SAV) approach for gradient flows*, J. Comput. Phys., 353:407–416, 2018. 1

[43] Q. Cheng and J. Shen, *Multiple scalar auxiliary variable (MSAV) approach and its application to the phase-field vesicle membrane model*, SIAM J. Sci. Comput ., 40:A3982–A4006, 2018. 1